KAUNAS UNIVERSITY OF TECHNOLOGY
CIVIL ENGINEERING AND ARCHITECTURE FACULTY

Mariana Putzolu

FLEXURAL REINFORCED CONCRETE MEMBER WITH FRP REINFORCEMENT

Master's Degree Final Project

Supervisor
Assoc. prof. dr. Mindaugas Augonis

KAUNAS, 2017

KAUNAS UNIVERSITY OF TECHNOLOGY
CIVIL ENGINEERING AND ARCHITECTURE FACULTY

FLEXURAL REINFORCED CONCRETE MEMBER WITH FRP REINFORCEMENT

Master's Degree Final Project
Civil Engineering (621H20001)

Supervisor
Assoc. prof. dr. Mindaugas Augonis
(19/05/2017)

Reviewer
Assoc. prof. dr. Juozas Vaiciunas
(19/05/2017)

Project made by
Mariana Putzolu
(19/05/2017)

KAUNAS,2017

KAUNAS UNIVERSITY OF TECHNOLOGY

Civil Engineering and Architecture Faculty

(Faculty)

Mariana Putzolu

(Student's name, surname)

Civil Engineering

(Title of study programme, code)

"Flexural Reinforced Concrete Member with FRP Reinforcement"

DECLARATION OF ACADEMIC INTEGRITY

19 May 2017

Kaunas

I confirm that the final project of mine, **Mariana Putzolu**, on the subject "Flexural Reinforced Concrete Member with FRP Reinforcement" is written completely by myself; all the provided data and research results are correct and have been obtained honestly. None of the parts of this thesis have been plagiarized from any printed, Internet-based or otherwise recorded sources; all direct and indirect quotations from external resources are indicated in the list of references. No monetary funds (unless required by law) have been paid to anyone for any contribution to this thesis.I fully and completely understand that any discovery of any facts of dishonesty inevitably results in me incurring a penalty under procedure effective at Kaunas University of Technology.

Mariana Putzolu

TABLE OF CONTENT

Mariana, Putzolu. Flexural Reinforced Concrete Member with FRP reinforcement.

Master's Final Project / supervisor assoc. prof. dr. Mindaugas Augonis; Faculty of Civil Engineering and Architecture, Kaunas University of Technology. Structure department.

Keywords: Analysis, FRP, fibers.

Kaunas, 2017.

SUMMARY

One of the most problematic point in construction is the durability of the concrete especially related to corrosion of the steel reinforcement. Due to this problem the construction sector, introduced the use of Fiber Reinforced Polymer, the main fibers used in construction are Glass, Carbon and Aramid. In this study, the author aim to analyse the flexural behaviour of concrete beams reinforced with FRP. This aim is achieved by the analysis of specimens reinforced with GFRP bars, with theoretical calculations of deflections and comparing the results with the experimental data from the literature. With the theoretical calculations, the main problems are the conservative results obtained from them if compared to the experimental data.
To compensate this difference has been used a coefficient of 0.75 in the cracked section moment of inertia to decrease this value obtaining a more coincident results compared to the experiment one.

Putzolu, Mariana. Lenkiamos kompozitine armatūra armuotos gelžbetoninės konstrukcijos. Magistro baigiamasis projektas / vadovas doc. dr. Mindaugas Augonis. Kauno technologijos universitetas, Statybos ir architektūros fakultetas.
Mokslo kryptis ir sritis: technologijos mokslai, statybos inžinerija.
Reikšminiai žodžiai: analizė, FRP, pluoštas
Kaunas, 2017, 65 p.

SANTRAUKA

Viena iš labiausiai probleminių vietų statyboje yra betono ilgaamžiškumas, ypač visa kas susiję su plieno armatūros korozija. Sprendžiant šią problemą statybų sektorius pristatė pluoštu armuoto polimero naudojimą. Pagrindiniai pluoštai, naudojami statybose yra stiklas, anglis ir aramidas. Šiame tyrime, autorius siekia išanalizuoti lenkiamų betono sijų sutvirtintų FRP, elgesį. Šis tikslas pasiekiamas bandinių, sutvirtintų GFRP barais, analize, su teoriniais įlinkių skaičiavimais ir lyginant rezultatus su eksperimentiniais duomenimis. Su teoriniais skaičiavimais, pagrindinės problemos yra konservatyvūs rezultatai gauti iš jų, lyginant su eksperimentiniais duomenimis. Tam, kad kompensuoti šį skirtumą, buvo naudojamas 0,75 koeficientas inercijos momentui plyšio vietoje turint tikslą sumažinti šį dydį gaunant daugiau sutampančių rezultatų lyginant su eksperimentu.

Introduction

The use of fiber-reinforced polymer (FRP) in concrete structures has increased rapidly in the last 20 years due to the excellent corrosion resistance, high tensile strength and good non – magnetization properties.

High strength and modulus fibers commonly used in composite materials are divided in three groups:

- polymeric fibers
- carbon fibers
- other inorganic fibers

The first group has one-dimensional primary bonds that is aligned with the longitudinal axis of the fibers.

The second group has two-dimensional sheets of graphite in a hexagonal planar network of primary bonds, aligned parallel to the axis fiber while the secondary bond is connecting the sheet in the radial direction of the fiber.

The third group has three-dimensional network of primary bonds due to provide strength and stiffness and a good thermal stability. [1]

The shape the surface, strength and stiffness of the fibers are influencing the mechanical properties of the composites [2] in particular by the tenacity and the tensile modulus, and some geometric parameters, such as:

• shape

• length;

• equivalent diameter;

• aspect ratio.

The aspect ratio is defined as the ratio, between the length of the fiber and its equivalent diameter. With the same composition and dosage, effectiveness of the fibers is improved by increasing the aspect ratio and if the form does an irregular contour that promotes the adhesion to the cement matrix.

The common used fibers are glass, carbon, aramid and basalt.

Glass fiber: They are made from silica sand and they are available in different grades. Mostly they are electrical E-glass, high strength S-glass and alkali-resistant AR-glass. Composite made by fiber glass showed a good electrical and thermal insulation properties.[3]

Carbon fiber: They are made from polycrylonitrile (PAN), pitch or rayon fiber. PAN based is the mostly used in civil engineering application.[3]

Aramid fiber: They are made from aromatic polyamide organic fibers. It has good mechanical properties and low-density high impact resistance. It is a good insulator and resists to organic solvents. His tensile strength and the modulus are higher than that from glass fibers .The most common type of aramid fiber is Kevlar. [3]

Basalt fiber: These fibers are stronger and stiffer than E-glass, safe, nontoxic, noncorrosive and nonmagnetic. Also if basalt is manufactured in the same way as E-glass the process for it requires less energy, and the primary material basalt is available everywhere. [3]

Comparison of Fiber Properties and Selected Metal

Material	Tensile Strength, 10^3 psi (MPa)	Tensile Modulus, 10^6 psi (GPa)	Density, lb/in.^{3} (g/cm^3)
Bulk 6061T6 Aluminum	45.0 (310)	10.0 (69)	0.098 (2.71)
Bulk SAE 4340 Steel	150.0 (1034)	29.0 (200)	0.283 (7.83)
E-glass fibers	500.0 (3448)	10.5 (72)	0.092 (2.54)
S-glass fibers	650.0 (4482)	12.5 (86)	0.090 (2.49)
Carbon fibers (PAN precursor)			
AS-4 (Hercules)	580.0 (4000)	33.0 (228)	0.065 (1.80)
IM-7 (Hercules)	785.0 (5413)	40.0 (276)	0.064 (1.77)
T-300 (Amoco)	530.0 (3654)	33.5 (231)	0.064 (1.77)
T-650/42 (Amoco)	730.0 (5033)	42.0 (290)	0.064 (1.77)
Carbon fibers (pitch precursor)			
P-55 (Amoco)	250.0 (1724)	55.0 (379)	0.072 (1.99)
P-75 (Amoco)	300.0 (2068)	75.0 (517)	0.072 (1.99)
P-100 (Amoco)	325.0 (2241)	100.0 (690)	0.078 (2.16)
Aramid fibers			
Kevlar® 29 (Dupont)	550.0 (3792)	9.0 (62)	0.052 (1.44)
Kevlar® 49 (Dupont)	550.0 (3792)	19.0 (131)	0.053 (1.47)
Boron fibers			
0.004" diameter (Textron)	510.0 (3516)	58.0 (400)	0.093 (2.57)
0.0056" diameter (Textron)	510.0 (3516)	58.0 (400)	0.090 (2.49)
Silicon carbide fibers			
0.0056" diameter (Textron)	500.0 (3448)	62.0 (427)	0.110 (3.04)

Figure 1 Comparison of fiber properties

The addition of fibers of any type and form is not able to affect the mechanical resistance to compression and the elastic modulus of the cementitious materials. However, a suitable dosage of fiber, especially if metal type, can affect the stress-strain behavior of a sample of concrete in a crushing test, making longer and less steep the downturn of the curve σ compression -ε for the action of stitching exerted by the fibers in respect of the slots that are produced in the direction orthogonal to that of maximum compression.

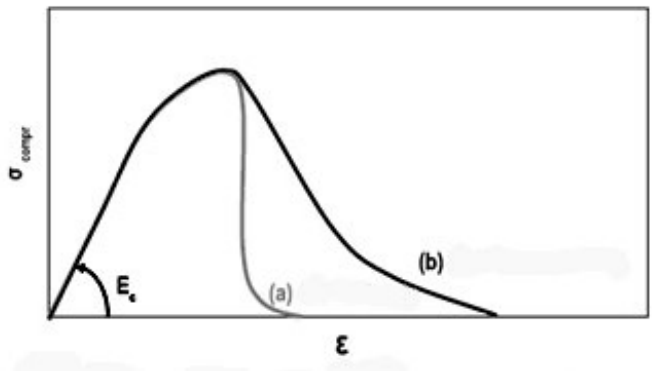

Figure 2 Compression stress-strain behavior of a) ordinary concrete b) fiber reinforced concrete

Depending on the dosage of fibers used, is possible to have two different behaviors post-cracking. For low fiber content (indicatively by volume of fibers of less than 2%) the behavior is softening. This means that after the crack, the material is able to support tensile stresses but they should be inferior to the one that caused the cracking of the matrix. In this case, in the specimens fiber-reinforced in the absence of other reinforcement, it forms a single slot, which increases in amplitude until the collapse as shown in part A of the Fig. 3.

For high dosage of fibers (indicatively by volume of fibers greater than 2%), the behavior post-crack FRC can be of hardening type. This means that in the mix it occurs a series of cracks that reach a stress higher than that, which produced the first lesion, part B Fig. 3. With the volume of fibers used in the most common applications, the tensile behavior of a fiber-reinforced concrete is, generally, of the softening type.

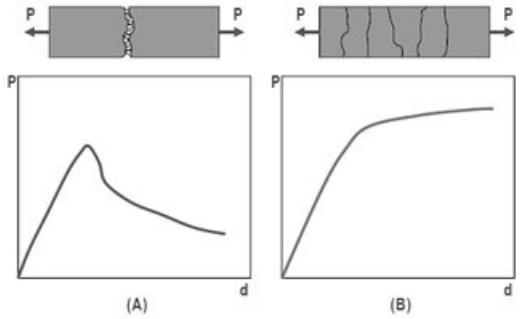

Figure 3 Behaviors of fiber-reinforced concrete under a load P.

Downturn behavior in A, hardening behavior in B.

1. FRP composite

The fiber reinforced polymer FRP are materials composed by longs resistant fibers impregnated in polymer usually resins. The main aim of the fibers is to be the resistant element while the polymer should protect the fibers from the external damages and ensure a good distribution of the stress uniformly. This concept can be found also in the ancient time, when the straw was used above the brick, is it possible to say that the use of FRP composite is an evolution of the old idea.

The aerospace used FRP composite for the law weight properties and for the high resistances. The problem of corrosion in the normal reinforced concrete bring the FRP material as a possible solution. The main properties of the FRP material are non-corrosive, lightweight and non-electromagnetic.

For the normal reinforced concrete in the beginning, the steel is protected from the concrete, but due to the external agents as humidity, will create rust and then corrosion. In this way, a constant maintenance is necessary to increase the life of the structure. The addition of the polymer reinforcement instead of the steel reinforcement will be more expansive, but, if related to the lifetime of a structure or to the benefits received from the utilization, the high cost will be afforded.

2. Composite materials and characteristic

The composite material are create by two different parts. The FRP are composed by:

- fibers: material anisotropic is the reinforcement ;
- matrix: a polymeric material.

Figure 4 Fibers

Each component is playing his rules in the composite.

2.1 Fiber phase

The rule of the fibers is to give the strength and stiffness [4], the fiber is the resistant material in the composite. The modulus of elasticity of the fiber is high, usually are made by thin filaments, connected between each other creating a texture as you can see in the Fig.5.

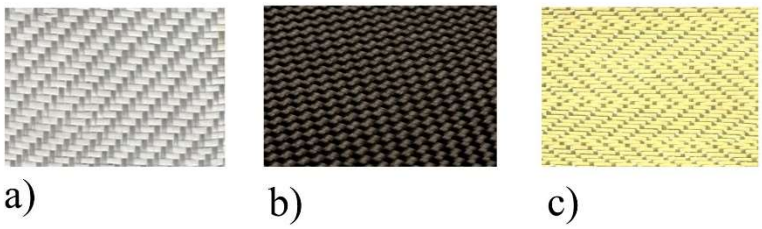

Figure 5 a) Glass texture b) Carbon texture c) Aramid texture

The particular shape give to the material rigidity and strength higher than the material itself used in different shape. Due to the dimension of the fibers, short or long there will be different behaviour of the material. The fibers are made by thin continuous filament the diameter is around 10^{-6} m.

As the filament of the fiber is so thin is not possible to manipulate them one by one, for this reason they are available in different shape (Fig.6) [12]:

- monofilament: base element with 10 μm diameter;
- tow: is made by machine consists in a bundle of filament and it will be used as discontinuous fiber;
- spun yarn: is made by the torsion of the fibers;
- roving: is a bundle of parallel spun yarn.

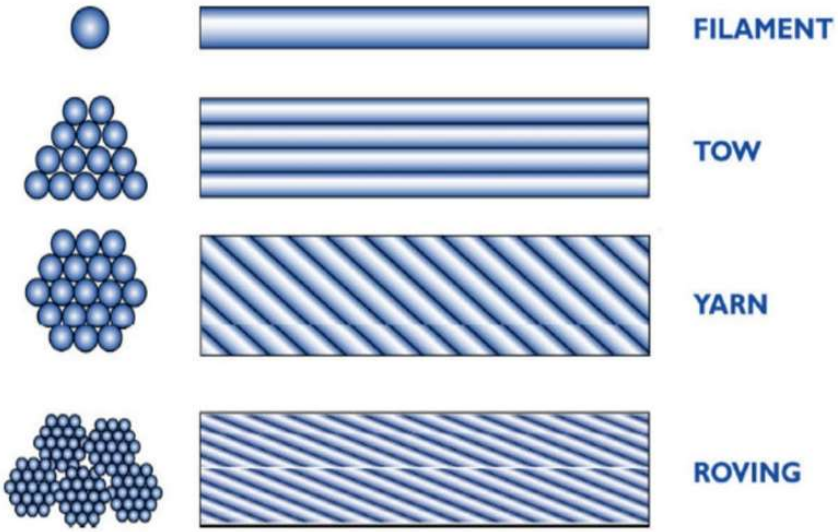

Figure 6 Type of fiber available on the market.

2.1.1 Main fibers for composite material

There are many kinds of fibers used. Further, there will be a description of the principle family of fibers used in civil engineering; a composite material can be made from two or more fibers.

The main fibers are:

- glass fibers;
- carbon fibers;
- aramid fibers.

2.1.2 Glass fibers

Glass fiber are a successful alternative with numerous advantages over traditional reinforcement.

The glass rebar is made of high strength and corrosion resistant glass fibers impregnated and bound by a durable polymeric resin.

The properties are ideal for any corrosive environments due to the resistance to chemical acids and alkaline bases. They improve the longevity of engineering structures where corrosion is a major factor.

Due to the change in the mix there are different class of Fiber Glass:

- E-Glass : alumino-borosilicate glass;
- S-Glass : alumino silicate glass with high magnesium;
- C-Glass : alkali-lime glass with high boron oxide;
- AR-Glass : Alkali Resistant glass made with zirconium silicates.

The main characteristic of different type of fiber are resumed in the Tab.1.

Table1-main fiber characteristic

Fiber type	**Modulus of elasticity**	**Tensile strength**	**Deformation**	**Operation temperature**
	(GPa)	(GPa)	%	(C°)
E-GLASS	72	3.5	4.4	550
S-GLASS	85	4.8	5.3	650
C-GLASS	69	3.3	4.8	600
AR-GLASS	55	2.5	4.7	477

The main properties of Glass fibers are:

- lighter in weight than the equivalent strength of Steel rebar;
- non-conductive to heat and electricity
- non-magnetic (transparent to electrical fields)
- non-existent corrosion, rust free
- transparent to radio frequencies
- impervious to chloride ion, low pH chemical attack and bacteriological growth
- low carbon footprint
- easy and Rapid Installation

Figure 7 Fiberglass bars

2.1.3 Carbon fibers

The carbon fibers starts to be used in the aerospace sector due to the need of a low weight and high strength material. In civil engineering and construction industry, this material can be useful in all the cases including deterioration and strengthening problems. This type of fibers are carbon elements prepared by pyrolysis of organic fibers, produced at 1315 °C.

In the main characteristic, we may find low density, good thermal insulation and good resistance to temperature changes.

The FRP made by carbon fiber are identified as CFRP.

The main properties of carbon fibers are:

- high resistance;
- low deformability;
- low impact resistance;
- high resistance to chemical agents.

2.1.4 Aramid fibers

They are created from polyamide organic fibers. The main properties are good mechanical behaviour, low-density high impact resistance. This material is a good insulator and resist to solvents. The tensile strength and modulus are higher than glass fibers. The common type of aramid fiber is Kevlar. [3]

The FRP made by aramid fibers are recognized as AFRP.

The main properties are:

- Non-linear;
- Good resistance to chemical agents;
- Low electric conductivity;

In the graph is possible to see the different behaviour of the different fibers.

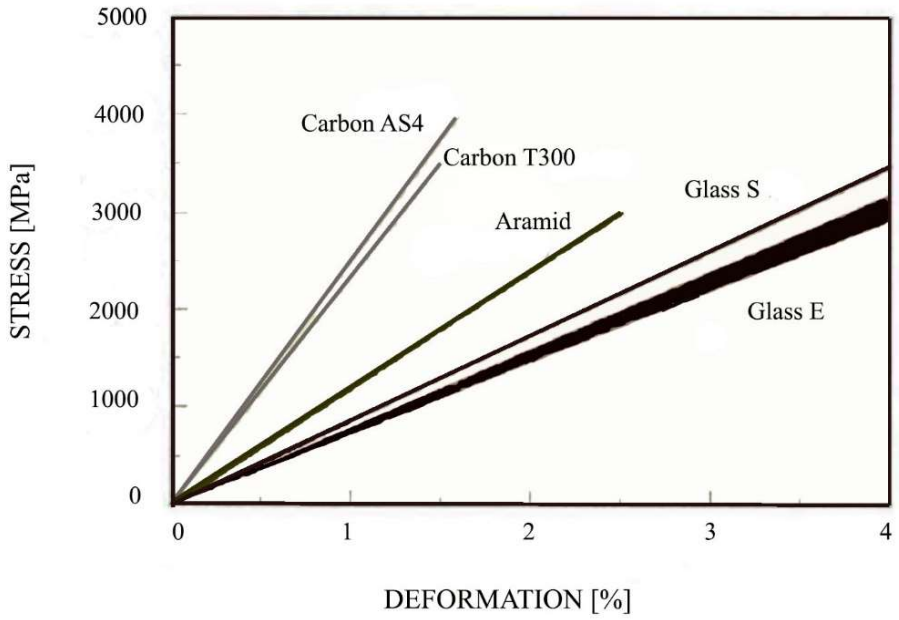

Figure 8 Different tensile stress behaviour of the fiber.

2.2 Matrix

The matrix give the good adherence to the fibers and distribute the stresses along the bar, isolating from deterioration due to the chemical agents.

The main properties that the matrix should have are:

- resistance to rupture bigger than fibers;
- all the fibers should be separated to don't let any opening appear;
- they should be chemical and thermal compatible with the fibers.

The matrix is a synthetic product from polymers mostly organic.

The matrix are classified as thermosetting and thermoplastic matrices.

- thermosetting resins are made by a chemical process called resin curing , those kind of resins are the most used due to the low processing temperature and the more convenient price[8].
- thermoplastic did not create any cross-linking chemical process. They are made by entanglement this is not a irreversible process so by heating they can be detangled and became a viscous fluid this process may damage the long fiber.

Therefore, this kind of matrix are more easily reparable but are more expansive and they need a bigger amount of energy to be created [7].

3 FRP Bars

Just at the end of 1980, the FRP bars became accessible as internal reinforcement for structures due to request of non-magnetic bars. They are composed, from two material fibers and polymers. The fibers are giving the strength and stiffness while the polymer is providing the protection and transferring the stresses [4].

The mechanical properties of FRP bars are different from the properties of steel bars. FRP bars are until the failure anisotropic linear and elastic, and also characterizes by high tensile strength just in the direction of the fibers [9, 10]

FRP bars are anisotropic, the strength and the stiffness depends from the type, the ratio and the volume of fibers, while the failure mechanism and the toughness is up to the type of resins [4,5,6]. The two component are working together the fiber as forcing phase and the polymer as a matrix. The matrix is protecting the fibers from direct exposure and bonding the fibers allowing the transfer of the stresses [4]. Some of the advantages of the bars are due to the matrix and its properties such as thermal stability moisture resistance [7].

The FRP bars are anisotropic, along the direction of the fibers the strength and the stiffness of the bar are affected from the kinds and the ratio of fibers.

In addition, some others factors are affecting the properties of FRP such as fiber orientation, manufacturing process and quality control and rate of resin curing [4,5-6].

Different techniques are used to manufacture the bar as:

- pultrusion;
- braidtrusion.

The cross-section is round. After the resin the bar cannot be bended, this should be done during the manufacturing process [3].

How are create the rebar by pultrusion?

Pultrusion is a process used to create FRP rebar with a continuous length of FRP and a consistent cross-section. The process start with pulling a combination of Glass fiber that will provide the strength along the profile. The glass will pass into a resin bath commonly the resins are polyester or vinyl Esther than pigment for color filler for enhance the properties and catalyst to pass from a liquid to a solid form. The fiber are than passing in the forming & curing Die the hit will let the fiber harden to create a solid rigid profile in the requested shape, than the profile will pass under a cutter that will cut the profiles into the previously chosen length .

How are the bar created by braidtrusion?

Braidtrusion is a process divided in different zone. In the first zone the carbon fibers are loaded onto a creel for pultrusion, each spool is tensioned, so in this way the pultruded yarns stay straight and aligned, the yarn pass through guides made with smooth surface to don’t damage the fibers, the yarns than pass through the first impregnation with resins hardener mix.

In the second zone right after the first impregnation the yarns are pulled to the center of a braider in which there is a circular ring, that will aloud the braid to be impregnated with heated resins, this second impregnation provide in just one step, the combination of impregnation and braid form . The formed profile will pass under a series of ovens.

3.1 Material characteristics.

3.1.1 Physical properties

- **Density:**

  The density is ranging from 1.25 to 2.1 g/cm^3 one/six to one/four the one from steel.

- **Coefficient of thermal expansion:**

  This coefficient vary in the longitudinal and transverse direction due to the single phases of the composite (matrix, fibers).

  The longitudinal coefficient is related to the properties of fibers, while the transverse is related to the matrix [6].

In the Table 2 is possible to see the coefficient of thermal expansion for FRP and steel bars. Where the coefficient is with a minus it mean that, the material contract with increased temperature and expands in vice versa.

Table 2-Typical coefficients of thermal expansion for reinforcing bars

Direction	CTE, $\times 10^{-6}$/°F ($\times 10^{-6}$/°C)			
	Steel	GFRP	CFRP	AFRP
Longitudinal, α_L	6.5 (11.7)	3.3 to 5.6 (6.0 to 10.0)	–4.0 to 0.0 (–9.0 to 0.0)	–3.3 to –1.1 (–6 to –2)
Transverse, α_T	6.5 (11.7)	11.7 to 12.8 (21.0 to 23.0)	41 to 58 (74.0 to 104.0)	33.3 to 44.4 (60.0 to 80.0)

*Typical values for fiber volume fraction ranging from 0.5 to 0.7.

3.2 Mechanical properties and behavior

3.2.1 Tensile behavior

The behavior is of one type characterized by a linear elastic stress-strain relationship until the rupture. The strength and stiffness of a FRP bar depend on different factors [4].

As the bar are load carrying the ratio of the fiber volume to the overall volume affect the tensile properties [4]. The unit tensile strength of a bar can change due to the change of diameter. The tensile strength of some FRP bar have to be requested to the manufacturer.

3.2.2 Compressive behavior

Test on FRP showed that the compressive strength is lower than tensile strength [11]. The failure in FRP bar under compression can include fiber micro bulking, transverse tensile or shear failure. The failure depends on type of fibers, fiber volume fraction and type of resin.

In most of the cases, the compressive strength is higher in bars with high tensile strength.

3.2.3 Shear behavior

The FRP bars are weak in interlaminar shear due to the lake of reinforcement between the layers of fibers, so the interlaminar shear is governed by the matrix.

To improve this lake is possible use off-axis fibers. This can happened by braiding or winding in a transverse way to the main fiber, this is possible also in case of pultrusion with different mechanism [4].

3.2.4 Bond behavior

For the FRP the bond behavior depends on design, manufacturing process, mechanical properties and the environmental conditions [4].

To investigate the bond properties the main tests are pullout test, splice test etc.

3.3 Time behavior

3.3.1 Creep rupture

With this term is usual to describe the progressive reduction of resistance under load after a long time. This is a viscosity phenomenon influenced by environmental conditions as temperature and humidity [4]. The most susceptible fibers to creep rupture are the glass fiber.

3.4 Temperature and fire

In the structures where the fire resistance is necessary to maintain the structure integrity, it is not recommended to use FRP reinforcement, because while the concrete cannot burn without oxygen, the reinforcement inside will soften due to the high temperature.

The glass-transition temperature T_g is the temperature at which the polymer will soften after that temperature the elastic modulus is reduced. T_g depend on the type of resin but is in the interval 65 to 120 °C [13].

The tensile properties of the composite decrease due to the reduction of the force transfer between the fibers through bond to the resin.

Test results showed that at 250°C would reduce the tensile strength of GFRP and CFRP bars in excess of 20% [14].

3.5 Comparison between FRP and steel.

As is possible to see from Fig.9, in the beginning the behavior of deformation for FRP and steel bar is the same elastic and linear. The FRP under stress will react with a linear behavior until when the material will collapse and break this make the FRP fragile, while the steel will reach a point in which the material is resisting, with a constant deformation, until the break point, called plastic behavior. Is it easier to work with material with this kind of behavior because they will alert if a collapse is going to occur and it will not be a sudden rupture.

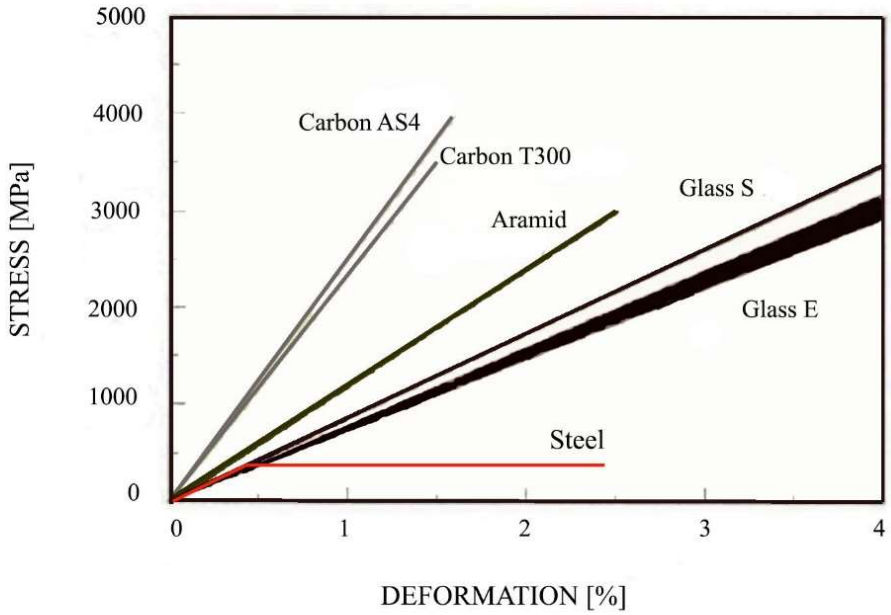

Figure 9 Comparison between FRP and steel

From the graph is it visible that the FRP mechanic resistance is greater than the steel material but is good to keep in mind the “fragile behavior”.

4. Analysis

4.1Notation

A_f = area of FRP reinforcement (mm2)

CE = environmental reduction factor for various fiber type and exposure conditions, given in Table 2.

E_c = modulus of elasticity of concrete (MPa)

E_f = design or guaranteed modulus of elasticity of FRP defined as mean modulus of sample of test specimens (Ef = Ef,ave) (MPa)

$f_{c'}$ = specified compressive strength of concrete (MPa)

f_f = stress in FRP reinforcement in tension (MPa)

f_{fu} = design tensile strength of FRP, considering reductions for service environment (MPa)

M_a = maximum momet in member at stage deflection is computed (Nmm)

M_{cr} = cracking moment (Nmm)

M_n = nominal moment capacity (N-mm)

n_f = ratio of modulus of elasticity of FRP bars

I_{cr} = moment of inertia of transformed cracked section (mm^4)

I_e = effective moment of inertia (mm^4)

I_g = gross moment of inertia (mm^4)

k = ratio depth neutral axis

β_d = reduction coefficient for deflection calculation

β_1 = factor taken as 0.85 for concrete strength fc′ up to and including 28 MPa. For strength above 28 MPa, this factor is reduced continuously at a rate of 0.05 per each 7 MPa of strength in excess of 28 MPa, but is not taken less than 0.65.

εc = strain in concrete

ε_{cu} = ultimate strain in concrete

b = width of rectangular cross section (mm)

d = distance from extreme compression fiber to centroid of tension reinforcement (mm)

ρ_f = FRP reinforcement ratio

ρ_{fb} = FRP reinforcement ratio producing balanced strain conditions

φ = strength reduction factor

Table 3 Environmental reduction factor for various and exposure condition.

Exposure condition	Fiber type	Environmental reduction factor C_E
Concrete not exposed to earth and weather	Carbon	1.0
	Glass	0.8
	Aramid	0.9
Concrete exposed to earth and weather	Carbon	0.9
	Glass	0.7
	Aramid	0.8

4.2 Analysis

This thesis presents an analytical study of the flexural behavior of concrete beams reinforced with FRP.

One of the most problematic point in construction is the durability of the concrete especially related to corrosion of the steel reinforcement.

One of the solutions, now a days is to use the FRP reinforcement as for example the glass fiber reinforced bars.

The stiffness of Glass Fiber Reinforced polymer bars is lower than steel reinforcement but they have high tensile strength with low elastic modulus.

This kind of bar have to be over reinforced so that they will fail by concrete crushing and not by fiber rupture. The GFRP bars have different properties, such as good fatigue behavior, high tensile strength, non-conductive and non-corrosive.

Indeed when they are used in flexural elements the tensile strength, the elastic modulus and the bond properties are governing the structural behavior of the elements.

The paper aims to analyze beams reinforced with Glass fiber bars by increasing the reinforcement ratio and further comparing the theoretical moment with the nominal moment capacity and calculating the moment of Inertia with several different equations to obtain the relative deflections based on the calculated moment of inertia.

The main formulas used for the calculation of the moment of Inertia are:

- Branson's equation adopted by ACI 440.1R-06 for the effective moment of intertia:

$$I_e = \left(\frac{M_{cr}}{M_a}\right)^3 \beta_d I_g + \left[1 - \left(\frac{M_{cr}}{M_a}\right)^3\right] I_{cr} \leq I_g \quad (1)$$

- Faza and GangaRao equation :

$$I_m = \frac{23 I_{cr} I_e}{8 I_{cr} + 15 I_e} \tag{2}$$

- Bischoff's equation :

$$I_e = \frac{I_{cr}}{1 - \left(1 - \frac{I_{cr}}{I_g}\right)\left(\frac{M_{cr}}{M}\right)^2} \tag{3}$$

For the calculation of the deflection :

$$\delta_{\max} = \frac{Pa}{48 E_c I_e}(3L^2 - 4a^2) \tag{4}$$

Where :

P= applied load

a= distance from supports

L= beam spam

E_c= modulus of elasticity

I_e= moment of inertia

4.3 Specimen description

The first tests are on beam reinforced with 2.80 m long GFRP bars with 12 mm diameter all the data for the bars is determined from ASTM Standards .The beam are 120 mm wide x 300 mm deep x 2800 mm long Fig.10, cast and test up to failure under four-point bending[16].

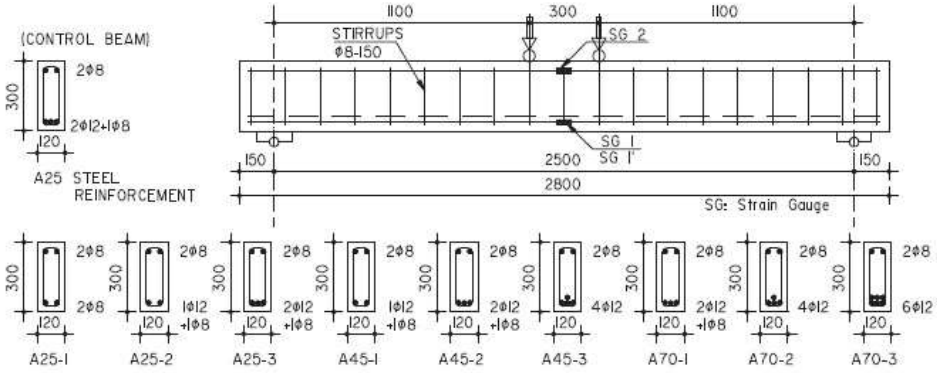

Figure 10 *Beams geometry and details*

The beams are designed as simple span with a proper amount of shear and longitudinal reinforcement to fail by GFRP rupture and concrete crushing.

The beams are identified as A-ll-z with the first term is intent to describe the group with the second the concrete strength and the last describe the specimen reinforcement. With number 1 the reinforcement ratio is equal to μ_b, number 2 equal to $1.7\mu_b$ and number 3 equal to $2.7\ \mu_b$.

μ_b is 0.33%, 0.54% and 0.92% for series A25, A45 and A70 respectively.

The specimens where tested under four-point bending, as showed in Fig. 10 the effective span 2500 mm, 1100 mm shear span, distance between loads 300 mm[16].

In the test the beams were observed, until the first crack appear recording the corresponding load. In TABLE 4 is showed a summary off the result.

TABLE 4 Test result

Series	*Beam specimen*	*Reinforcement Ratio*	*Initial Cracking load (Kn)*	*Failure Load (Kn)*
A25	A25-1	0.0032	10.2	45.9
	A25-2	0.0055	10.8	40.7
	A25-3	0.0088	10.9	75.2
A45	A45-1	0.0054	55.8	55.8
	A45-2	0.0091	81.9	81.9
	A45-3	0.0145	109.8	109.8
A70	A70-1	0.0092	84.6	84.6
	A70-2	0.0156	132.7	132.7
	A70-3	0.0248	145.1	145.1

4.4 Calculation

In the following tables 5-13, you can see the main information about the specimens, the difference between A25/A45/A70 is the compressive strength of concrete and the relative factor for concrete strength. For each class there are three main specimens with different reinforcement ratio.

Table 5. Specimen A25-1

Ef(Mpa)	Ɛcu	β1	f'c(Mpa)	pf	b(mm)	d(mm)	f*fu(Mpa)	Af(mm^2)	CE	Ɛfu	Ec Mpa
40.700	0,003	0,85	25	0,003277778	120	300	640	118	0,8	0,014	23750
40.700	0,003	0,85	25	0,003611111	120	300	640	130	0,8	0,014	23750
40.700	0,003	0,85	25	0,005	120	300	640	180	0,8	0,014	23750
40.700	0,003	0,85	25	0,005833333	120	300	640	210	0,8	0,014	23750
40.700	0,003	0,85	25	0,006388889	120	300	640	230	0,8	0,014	23750
40.700	0,003	0,85	25	0,008333333	120	300	640	300	0,8	0,014	23750

Table 6. Specimen A25-2

Ef(Mpa)	Ɛcu	β1	f'c(Mpa)	pf	b(mm)	d(mm)	f*fu(Mpa)	Af(mm^2)	CE	Ɛfu	Ec(Mpa)
40.700	0,003	0,85	25	0,00561	120	300	640	201,96	0,8	0,014	23750
40.700	0,003	0,85	25	0,006111	120	300	640	220	0,8	0,014	23750
40.700	0,003	0,85	25	0,007778	120	300	640	280	0,8	0,014	23750
40.700	0,003	0,85	25	0,008889	120	300	640	320	0,8	0,014	23750
40.700	0,003	0,85	25	0,01	120	300	640	360	0,8	0,014	23750
40.700	0,003	0,85	25	0,011111	120	300	640	400	0,8	0,014	23750

Table 7. Specimen A25-3

Ef(Mpa)	Ɛcu	β1	f'c(Mpa)	pf	b(mm)	d(mm)	f*fu(Mpa)	Af(mm^2)	CE	Ɛfu	Ec(Mpa)
40.700	0,003	0,85	25	0,008889	120	300	640	320	0,8	0,014	23750
40.700	0,003	0,85	25	0,009056	120	300	640	326	0,8	0,014	23750
40.700	0,003	0,85	25	0,010556	120	300	640	380	0,8	0,014	23750
40.700	0,003	0,85	25	0,011389	120	300	640	410	0,8	0,014	23750
40.700	0,003	0,85	25	0,011736	120	300	640	422,5	0,8	0,014	23750
40.700	0,003	0,85	25	0,012083	120	300	640	435	0,8	0,014	23750

Table 8. Specimen A45-1

Ef(Mpa)	Ɛcu	β1	f'c(Mpa)	pf	b(mm)	d(mm)	f*fu(Mpa)	Af(mm^2)	CE	Ɛfu	Ec(Mpa)
40.700	0,003	0,7	45	0,0054	120	300	650	194,4	0,8	0,014	31863,97
40.700	0,003	0,7	45	0,0061	120	300	650	220	0,8	0,014	31863,97
40.700	0,003	0,7	45	0,0068	120	300	650	245	0,8	0,014	31863,97
40.700	0,003	0,7	45	0,0078	120	300	650	280	0,8	0,014	31863,97
40.700	0,003	0,7	45	0,0089	120	300	650	320	0,8	0,014	31863,97
40.700	0,003	0,7	45	0,0097	120	300	650	350	0,8	0,014	31863,97

Table 9. Specimen A45-2

Ef(Mpa)	Ɛcu	β1	f'c(Mpa)	pf	b(mm)	d(mm)	f*fu(Mpa)	Af(mm^2)	CE	Ɛfu	Ec(Mpa)
40.700	0,003	0,7	45	0,00918	120	300	650	330,48	0,8	0,014	31863,97
40.700	0,003	0,7	45	0,009778	120	300	650	352	0,8	0,014	31863,97
40.700	0,003	0,7	45	0,010278	120	300	650	370	0,8	0,014	31863,97
40.700	0,003	0,7	45	0,011389	120	300	650	410	0,8	0,014	31863,97
40.700	0,003	0,7	45	0,011806	120	300	650	425	0,8	0,014	31863,97
40.700	0,003	0,7	45	0,012583	120	300	650	453	0,8	0,014	31863,97

Table 10. Specimen A45-3

Ef(Mpa)	Ɛcu	β1	f'c(Mpa)	pf	b(mm)	d(mm)	f*fu(Mpa	Af(mm^2)	CE	Ɛfu	Ec(Mpa)
40.700	0,003	0,7	45	0,01458	120	300	650	524,88	0,8	0,014	31863,97
40.700	0,003	0,7	45	0,014778	120	300	650	532	0,8	0,014	31863,97
40.700	0,003	0,7	45	0,015	120	300	650	540	0,8	0,014	31863,97
40.700	0,003	0,7	45	0,015556	120	300	650	560	0,8	0,014	31863,97
40.700	0,003	0,7	45	0,015778	120	300	650	568	0,8	0,014	31863,97
40.700	0,003	0,7	45	0,016667	120	300	650	600	0,8	0,014	31863,97

Table 11. Specimen A70-1

Ef(Mpa)	Ɛcu	β1	f'c(Mpa)	pf	b(mm)	d(mm)	f*fu(Mpa)	Af(mm^2)	CE	Ɛfu	Ec(Mpa)
40.700	0,003	0,55	70	0,0092	120	300	650	331,2	0,8	0,014	39741,35
40.700	0,003	0,55	70	0,0096	120	300	650	345	0,8	0,014	39741,35
40.700	0,003	0,55	70	0,0101	120	300	650	362	0,8	0,014	39741,35
40.700	0,003	0,55	70	0,0111	120	300	650	400	0,8	0,014	39741,35
40.700	0,003	0,55	70	0,0117	120	300	650	420	0,8	0,014	39741,35
40.700	0,003	0,55	70	0,0121	120	300	650	435	0,8	0,014	39741,35

Table 12. Specimen A70-2

Ef(Mpa)	Ɛcu	β1	f'c(Mpa)	pf	b(mm)	d(mm)	f*fu(Mpa)	Af(mm^2)	CE	Ɛfu	Ec(Mpa)
40.700	0,003	0,55	70	0,01564	120	300	650	563,04	0,8	0,014	39741,35
40.700	0,003	0,55	70	0,016111	120	300	650	580	0,8	0,014	39741,35
40.700	0,003	0,55	70	0,017222	120	300	650	620	0,8	0,014	39741,35
40.700	0,003	0,55	70	0,018056	120	300	650	650	0,8	0,014	39741,35
40.700	0,003	0,55	70	0,019444	120	300	650	700	0,8	0,014	39741,35
40.700	0,003	0,55	70	0,02	120	300	650	720	0,8	0,014	39741,35

Table 13. Specimen A70-3

Ef(Mpa)	Ɛcu	β1	f'c(Mpa)	pf	b(mm)	d(mm)	f*fu(Mp	Af(mm^2)	CE	Ɛfu	Ec(Mpa)
40.700	0,003	0,55	70	0,024833	120	300	650	894	0,8	0,014	39741,35
40.700	0,003	0,55	70	0,025	120	300	650	900	0,8	0,014	39741,35
40.700	0,003	0,55	70	0,025556	120	300	650	920	0,8	0,014	39741,35
40.700	0,003	0,55	70	0,02625	120	300	650	945	0,8	0,014	39741,35
40.700	0,003	0,55	70	0,026667	120	300	650	960	0,8	0,014	39741,35
40.700	0,003	0,55	70	0,027083	120	300	650	975	0,8	0,014	39741,35

The nominal flexural strength for FRP can be evaluated by the mode of failure. The flexural capacity for FRP member depends on the type of failures (FRP rupture or concrete crushing). This can be checked comparing the FRP reinforcement ratio with the balanced reinforcement ratio (this is the ratio in which, the FRP rupture and the concrete crush are at the same moment) Fig.11, is showed in Table 8, 9 and 10. According to ACI 440 a section is under concrete crushing when $\rho_f > 1.4\ \rho_{fb}$, while is a FRP rupture when $\rho_f < \rho_{fb}$.

In all the case in which the member are designed for FRP rupture, an amount of reinforcement have to be added to prevent the concrete crush.

$$\rho_f = \frac{A_f}{bd} \tag{5}$$

$$\rho_{fb} = 0.85\beta_1 \frac{f_c'}{f_{fu}} \frac{E_f \varepsilon_{cu}}{E_f \varepsilon_{cu} + f_{fu}} \tag{6}$$

Figure 11 Reinforcement ratio and balanced reinforcement ratio

Table 13. Reinforcement ratio A25-1

ρ_{fb}*1.4	ρ_{fb}	ρ_f		Φ
0,009958	0,007113	0,003278		0,55
0,009958	0,007113	0,003611		0,55
0,009958	0,007113	0,005		0,55
0,009958	0,007113	0,005833		0,55
0,009958	0,007113	0,006389		0,55
0,009958	0,007113	0,008333	concrete crush	0,592901686

Table 14. Reinforcement ratio A25-2

ρ_{fb} *1.4	ρ_{fb}	pf		Φ
0,009958	0,007113	0,00561	FRP rupture	0,55
0,009958	0,007113	0,006111		0,55
0,009958	0,007113	0,007778		0,573375
0,009958	0,007113	0,008889		0,612428
0,009958	0,007113	0,01		0,65
0,009958	0,007113	0,011111	concrete crush	0,65

Table 15. Reinforcement ratio A25-3

ρ_{fb} *1.4	ρ_{fb}	pf		Φ
0,009958	0,007113	0,008889		0,612428
0,009958	0,007113	0,009056		0,618286
0,009958	0,007113	0,010556	concrete crush	0,65
0,009958	0,007113	0,011389		0,65
0,009958	0,007113	0,011736		0,65
0,009958	0,007113	0,012083		0,65

Table 14. Reinforcement ratio A45-1

ρ_{fb}*1.4	ρ_{fb}	pf		Φ
0,017428	0,012449	0,0054	FRP rupture	0,55
0,017428	0,012449	0,006111		0,55
0,017428	0,012449	0,006806		0,55
0,017428	0,012449	0,007778		0,55
0,017428	0,012449	0,008889		0,55
0,017428	0,012449	0,009722		0,55

Table 15. Reinforcement ratio A45-2

ρ_{fb}*1.4	ρ_{fb}	pf		Φ
0,017428	0,012449	0,00918	FRP rupture	0,55
0,017428	0,012449	0,009778		0,55
0,017428	0,012449	0,010278		0,55
0,017428	0,012449	0,011389		0,55
0,017428	0,012449	0,011806		0,55
0,017428	0,012449	0,012583		0,5527

Table 16. Reinforcement ratio A45-3

ρ_{fb}*1.4	ρ_{fb}	p_f		Φ
0,017428	0,012449	0,01458	concrete crush	0,592797
0,017428	0,012449	0,014778		0,596769
0,017428	0,012449	0,015		0,601231
0,017428	0,012449	0,015556		0,612388
0,017428	0,012449	0,015778		0,616851
0,017428	0,012449	0,016667		0,634702

Table 17. Reinforcement ratio A70-1

ρ_{fb}*1.4	ρ_{fb}	ρ_f		Φ
0,027111	0,019365	0,0092	FRP rupture	0,55
0,027111	0,019365	0,009583		0,55
0,027111	0,019365	0,010056		0,55
0,027111	0,019365	0,011111		0,55
0,027111	0,019365	0,011667		0,55
0,027111	0,019365	0,012083		0,55

Table 18. Reinforcement ratio A70-2

ρ_{fb}*1.4	ρ_{fb}	ρ_f		Φ
0,027111	0,019365	0,01564	FRP rupture	0,55
0,027111	0,019365	0,016111		0,55
0,027111	0,019365	0,017222		0,55
0,027111	0,019365	0,018056		0,55
0,027111	0,019365	0,019444	Concrete crush	0,501911
0,027111	0,019365	0,02		0,507993

Table 19. Reinforcement ratio A70-3

ρ_{fb}*1.4	ρ_{fb}	ρ_f		Φ
0,027111	0,019365	0,024833	Concrete crush	0,620596
0,027111	0,019365	0,025		0,622748
0,027111	0,019365	0,025556		0,62992
0,027111	0,019365	0,02625		0,638885
0,027111	0,019365	0,026667		0,644264
0,027111	0,019365	0,027083		0,65

The design flexural strength have to be bigger than the factored moment.

$$\Phi M_n \geq M_u \qquad (7)$$

For the FRP, it is necessary to add a strength reduction factor to provide reserve of strength due to the fact that FRP members don't have a plastic behavior.

This factor Φ is equal to 0.65 for concrete rupture and 0.55 for FRP rupture

The nominal moment M_n have different forms. When $\rho_f > \rho_{fb,}$ the failure is initiated by concrete crushing and the flexural strength is calculated based on the following equation:

$$M_n = \rho_f f_f \left(1 - 0.59 \frac{\rho_f f_f}{f'_c}\right) bd^2 \tag{8}$$

When $\rho_f < \rho_{fb}$ the failure is by FRP rupture. Then the nominal flexural strength can be calculated as follows:

$$M_n = A_f f_{fu} \left(d - \frac{\beta_1 c_b}{2}\right) \tag{9}$$

For all the specimens Eq.(7) is analyzed and proved.

The nominal moment, was calculated also with a theoretical formula in which is added a reduction factor to the ultimate tensile strength of FRP[15]. This equation has been compared with Eq. (8-9) as showed in Fig. 13-15.

$$\mathbf{M_{theo} = 0.50 A_p f_{pu} d \left(1 - 0.30 p \frac{f_{pu}}{f_c}\right)} \tag{10}$$

The comparisons are showed in the following figures.

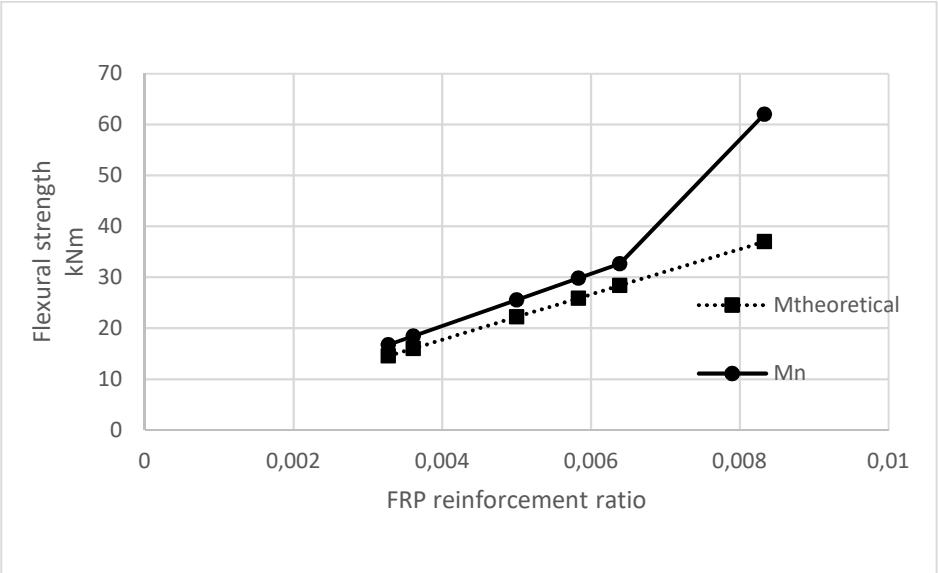

Figure 12 Comparison between theoretical and experimental nominal moment specimens A25-1

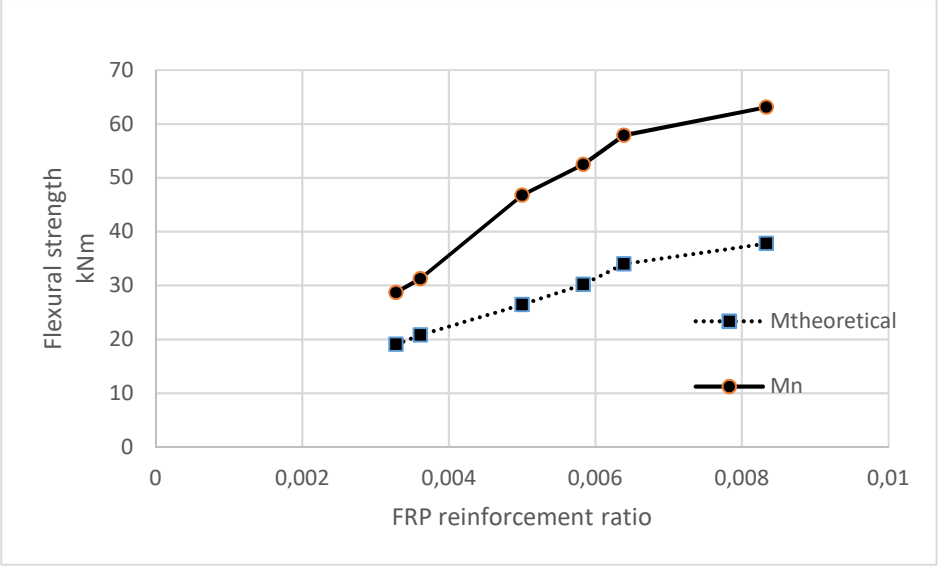

Figure 13 Comparison between theoretical and experimental nominal moment specimens A25-2.

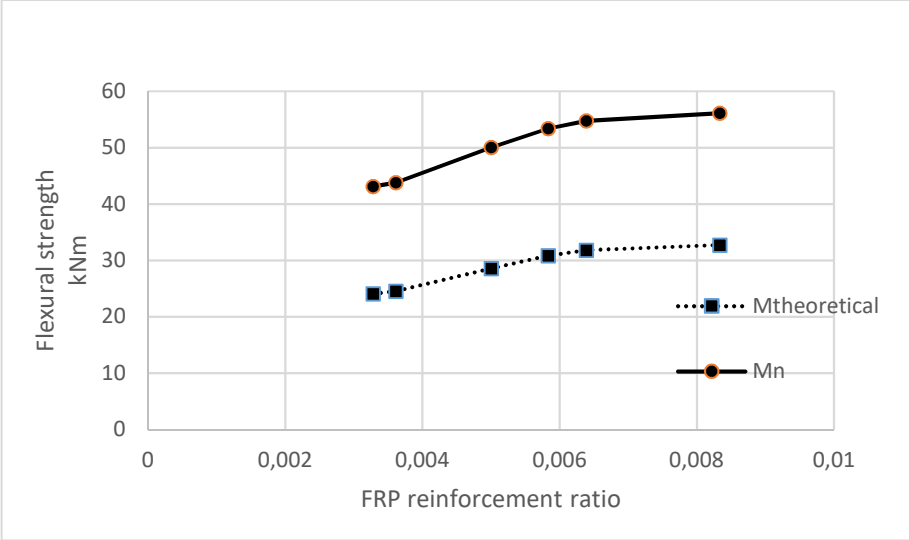

Figure 14 Comparison between theoretical and experimental nominal moment specimens A25-3.

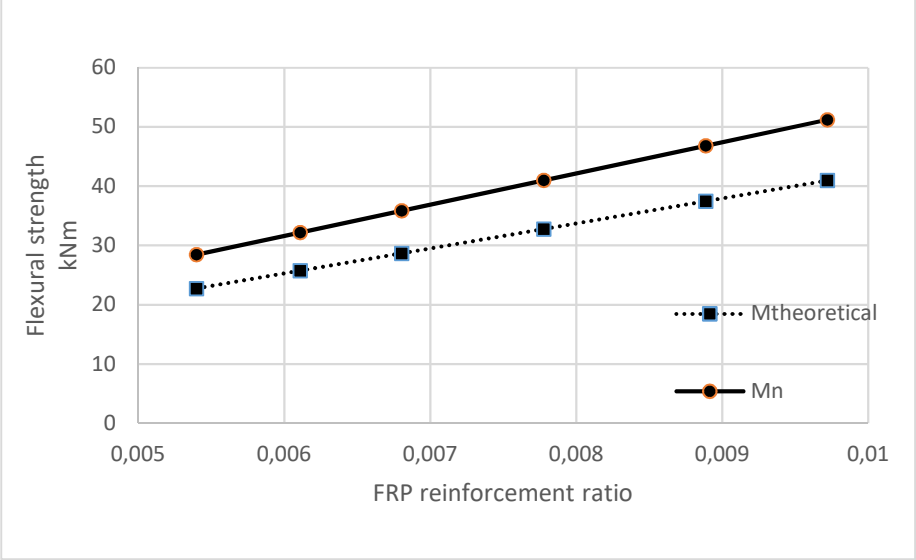

Figure 15 Comparison between theoretical and experimental nominal moment specimens A45-1.

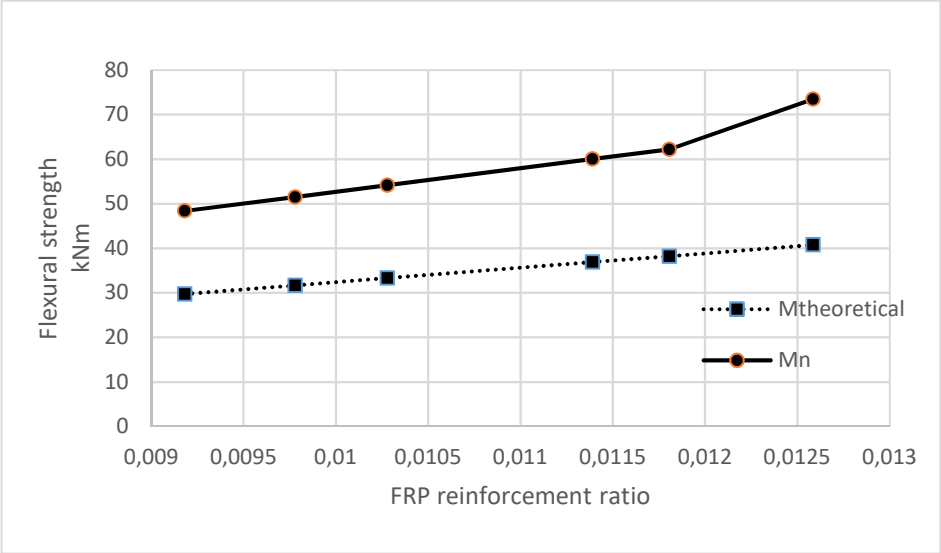

Figure 16 Comparison between theoretical and experimental nominal moment specimens A45-2.

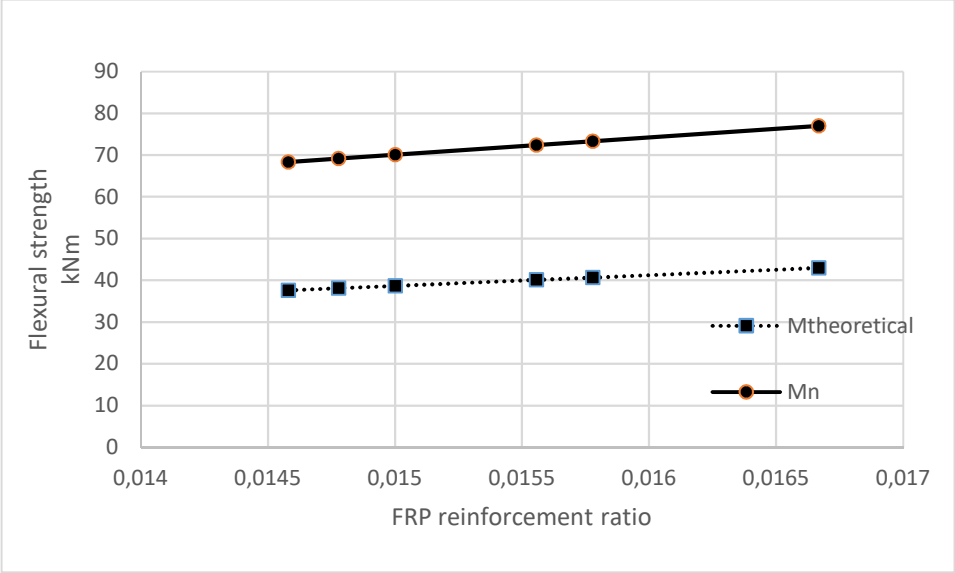

Figure 17 Comparison between theoretical and experimental nominal moment specimens A45-3.

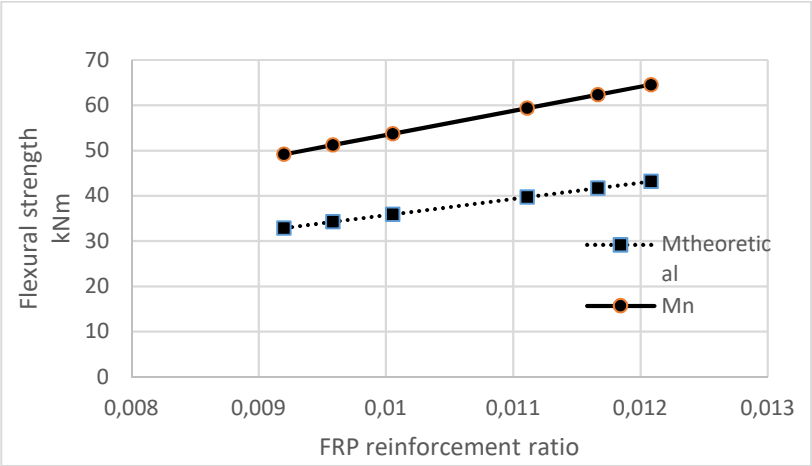

Figure 18 Comparison between theoretical and experimental nominal moment specimens A70-1.

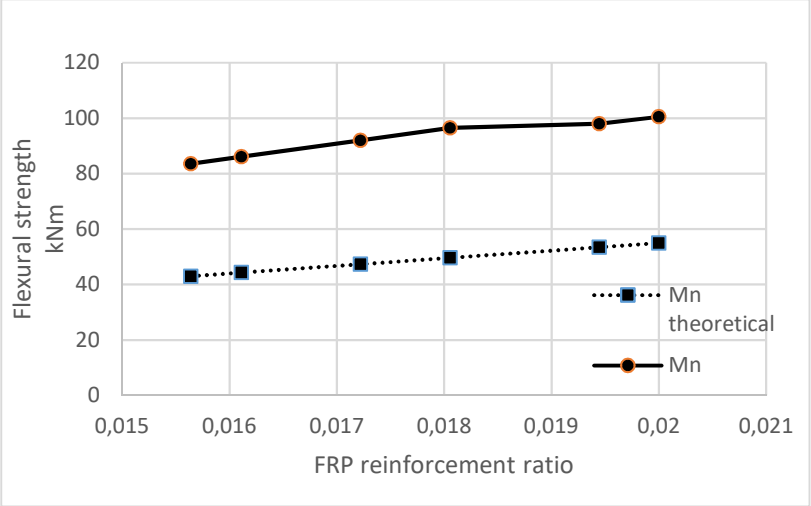

Figure 19 Comparison between theoretical and experimental nominal moment specimens A70-2.

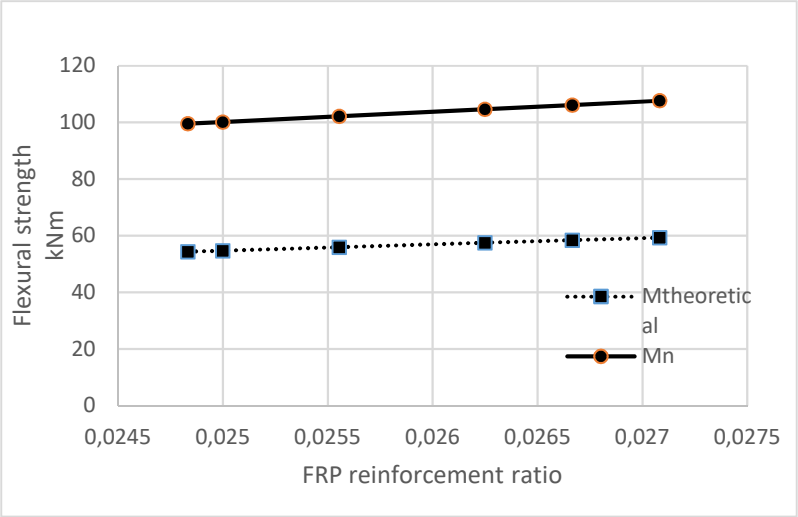

Figure 20 Comparison between theoretical and experimental nominal moment specimens A70-3.

4.4.1 Moment of Inertia

The next step is the calculation of the moment of inertia, the first equation used is :

$$I_e = \left(\frac{M_{cr}}{M_a}\right)^3 I_g + \left[1 - \left(\frac{M_{cr}}{M_a}\right)^3\right] I_{cr} \leq I_g \tag{10}$$

Branson's equation adopted from ACI 318- 05, based on steel-reinforcement behavior, represents an effective moment of inertia (I_e) that change from the gross moment of inertia (I_g) to the moment of inertia based at the cracking section (I_{cr}) as it increase the load on the member before the cracking point.[4]

$$I_e = \left(\frac{M_{cr}}{M_a}\right)^3 \beta_d I_g + \left[1 - \left(\frac{M_{cr}}{M_a}\right)^3\right] I_{cr} \leq I_g$$

ACI.1R-06 modify this equation including a reduction factor β_d due to the reduced tension stiffening of FRP.

$$\beta_d = \left(\frac{1}{5}\right) * \left(\frac{\rho f}{\rho f b}\right)$$

This problem may be caused from the lower modulus of elasticity and different stress bond level in FRP members. [4]

The second equation is Faza and Ganga Rao this model is based on the fact that the concrete section between the loads point if cracked and the end sections just partially cracked

$$I_m = \frac{23 I_{cr} I_e}{8 I_{cr} + 15 I_e}$$

The third equation is Bischoff's is related to a moment of inertia based on the tension- stiffening effect on curvature :

$$I_e = \frac{I_{cr}}{1 - \left(1 - \frac{I_\sigma}{I_g}\right)\left(\frac{M_\sigma}{M}\right)^2}$$

The comparison between these three different equations is showed in Fig. 22-30

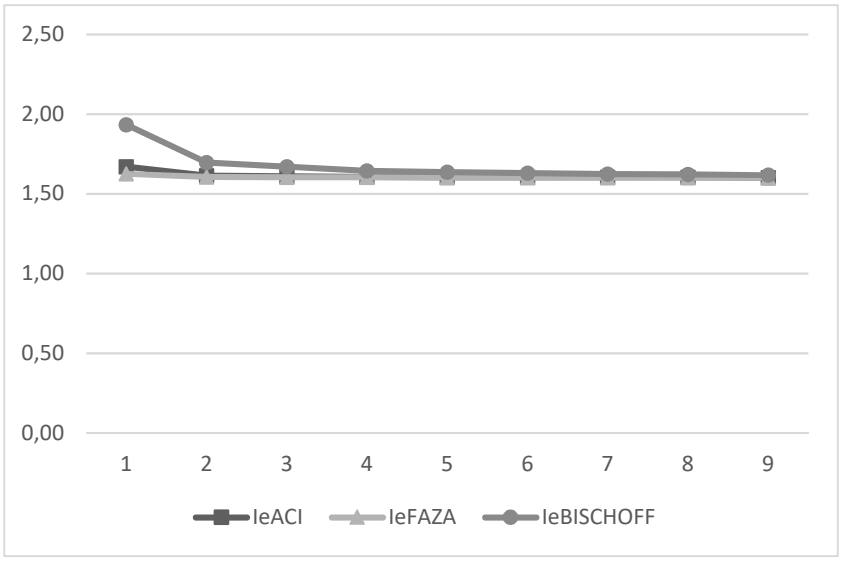

Figure 21 Comparison between different moment of inertia A25-1

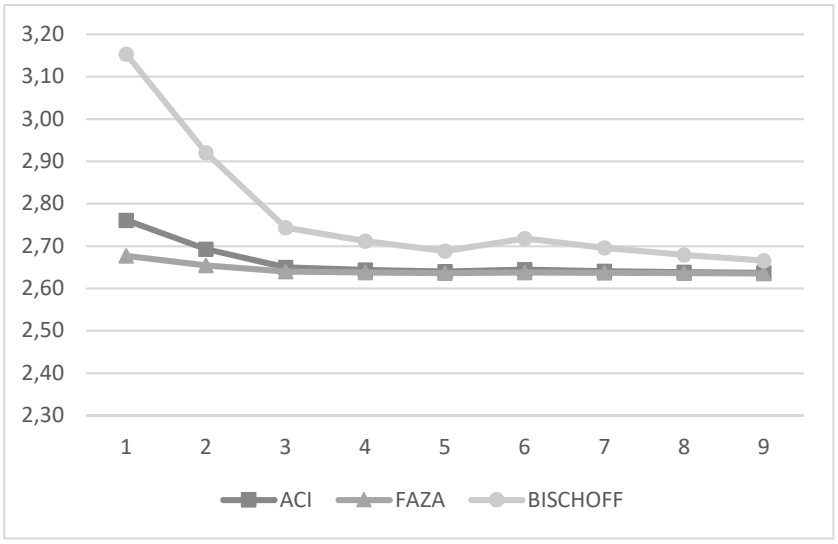

Figure 22 Comparison between different moment of inertia A25-2

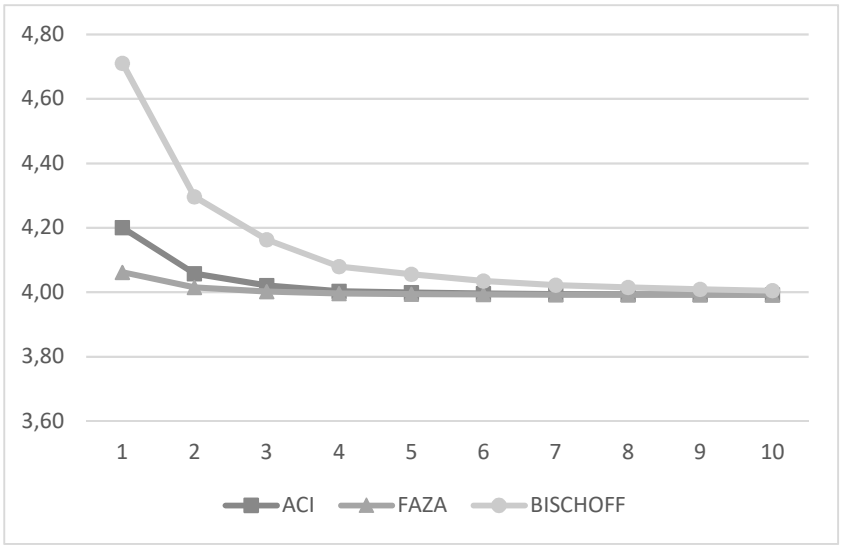

Figure 23 Comparison between different moment of inertia A25-3

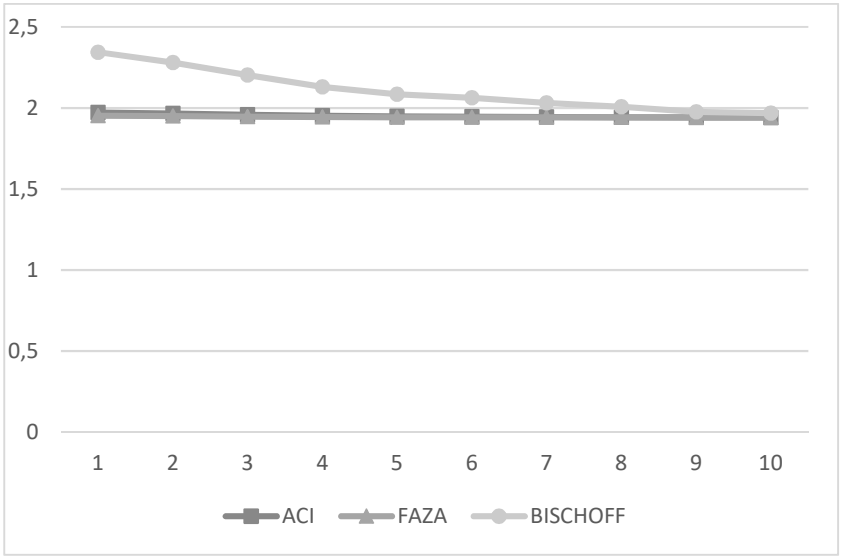

Figure 24 Comparison between different moment of inertia A45-1

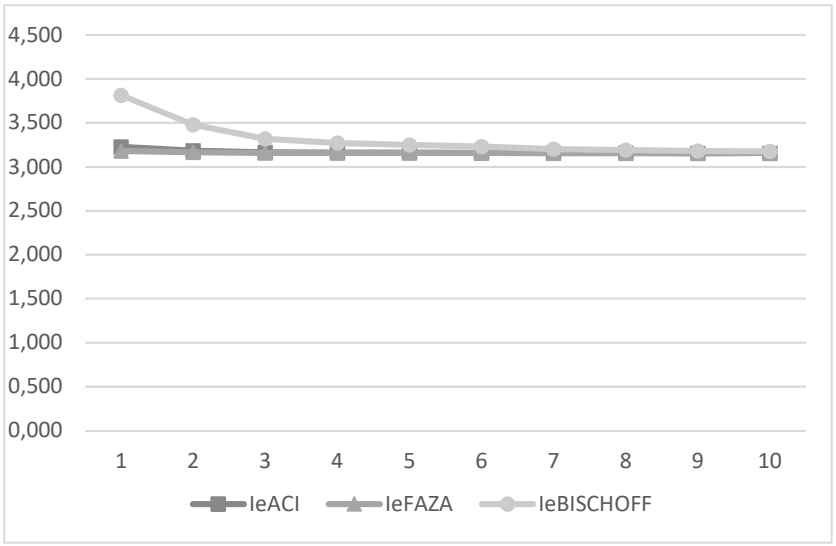

Figure 25 Comparison between different moment of inertia A45-2

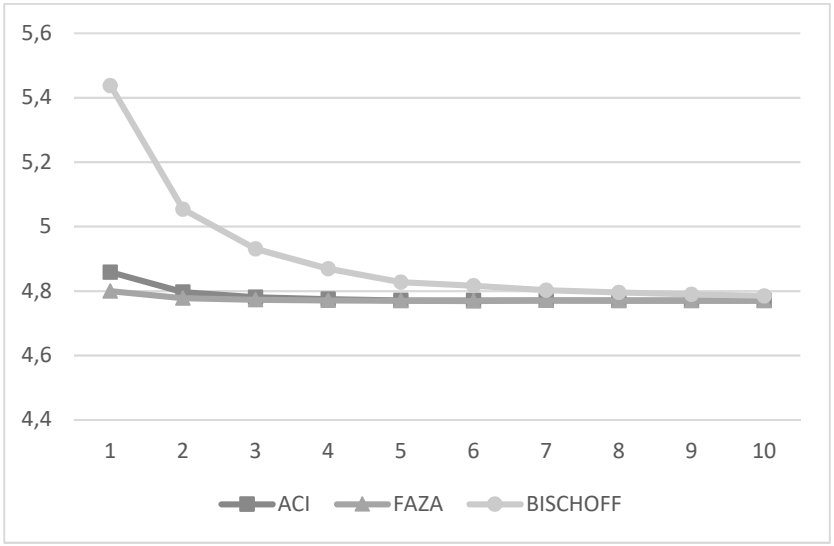

Figure 26 Comparison between different moment of inertia A45-3

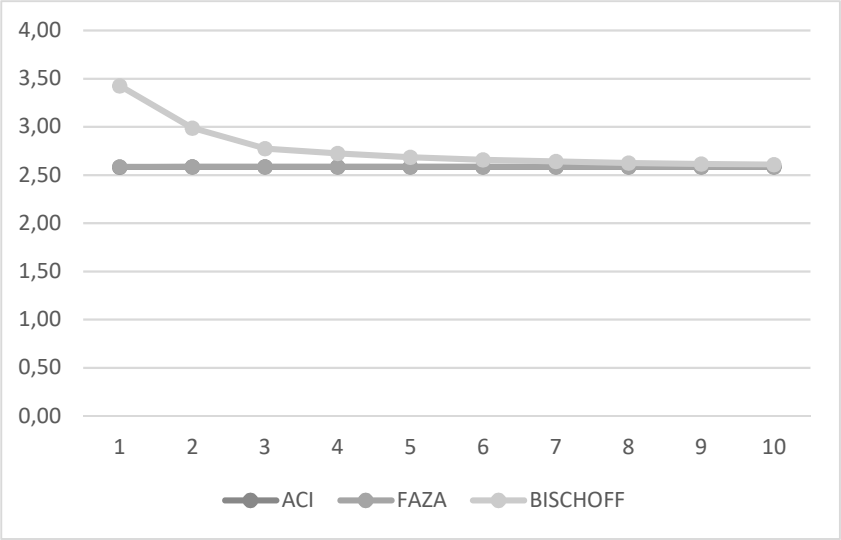

Figure 27 Comparison between different moment of inertia A70-1

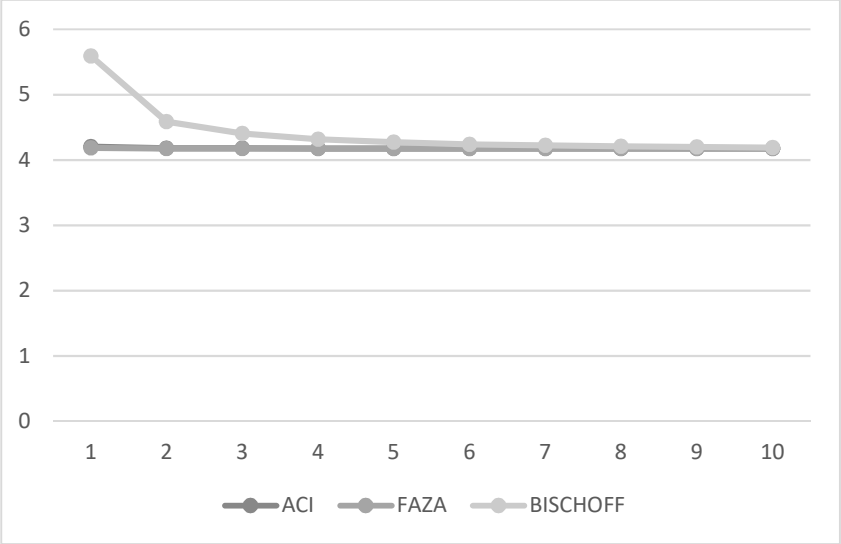

Figure 28 Comparison between different moment of inertia A70-2

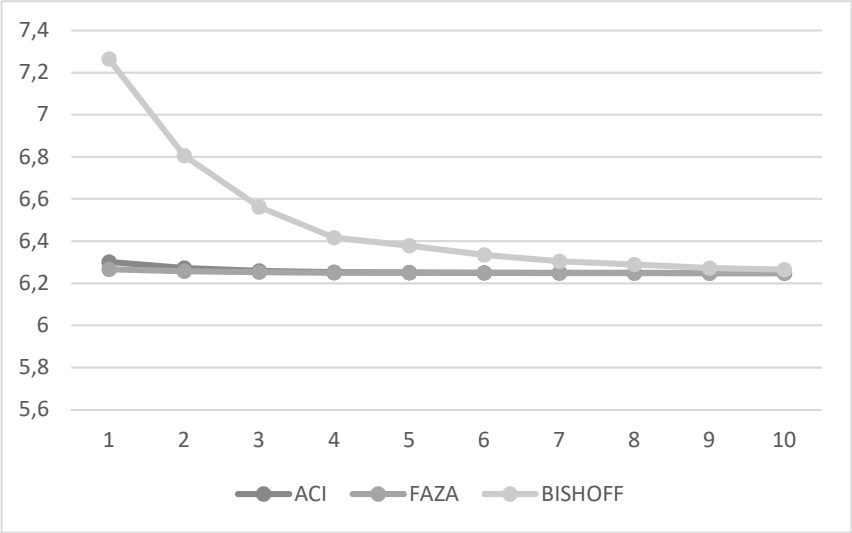

Figure 29 Comparison between different moment of inertia A70-3

All the series present different moment of inertia, the main difference between these theoretical equations is represented from BISCHOFF'S equation that have in the begging a higher value to end with mostly same result as the other equations.

4.4.2 Deflections

The maximum deflection is calculated by Eq. (5), for each single specimens with the different moments of inertia calculated before. All the results are showed in the following Fig. 31-39.

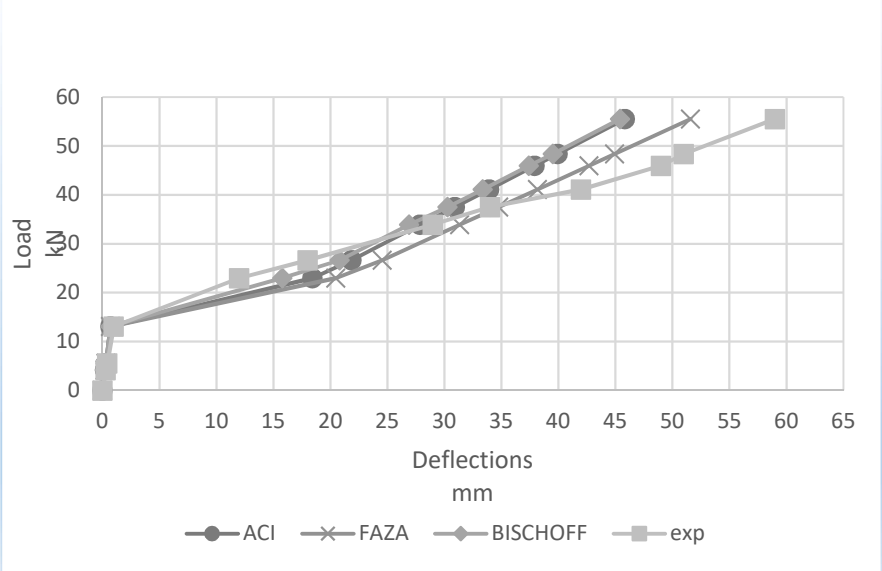

Figure 30 Comparison of deflections with different moment of inertia A25-1

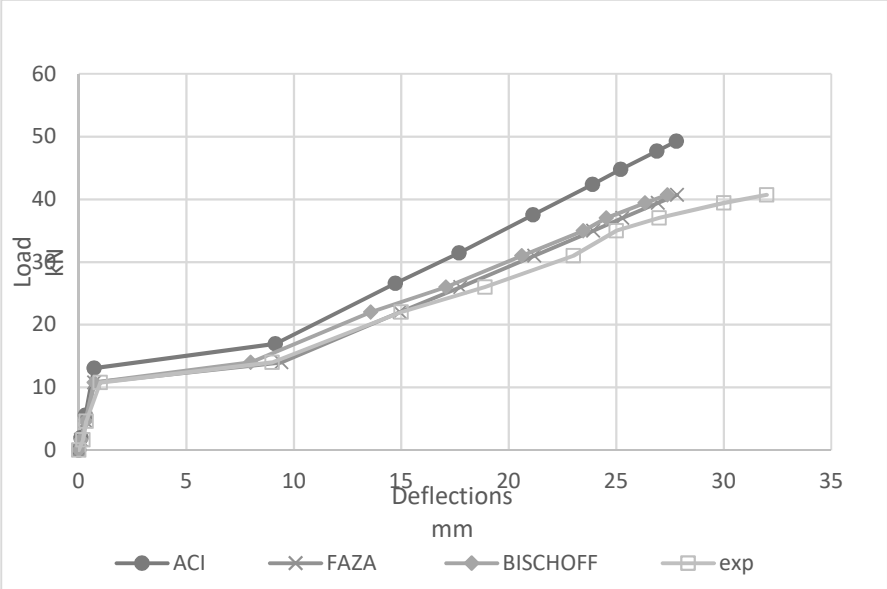

Figure 31 Comparison of deflections with different moment of inertia A25-2

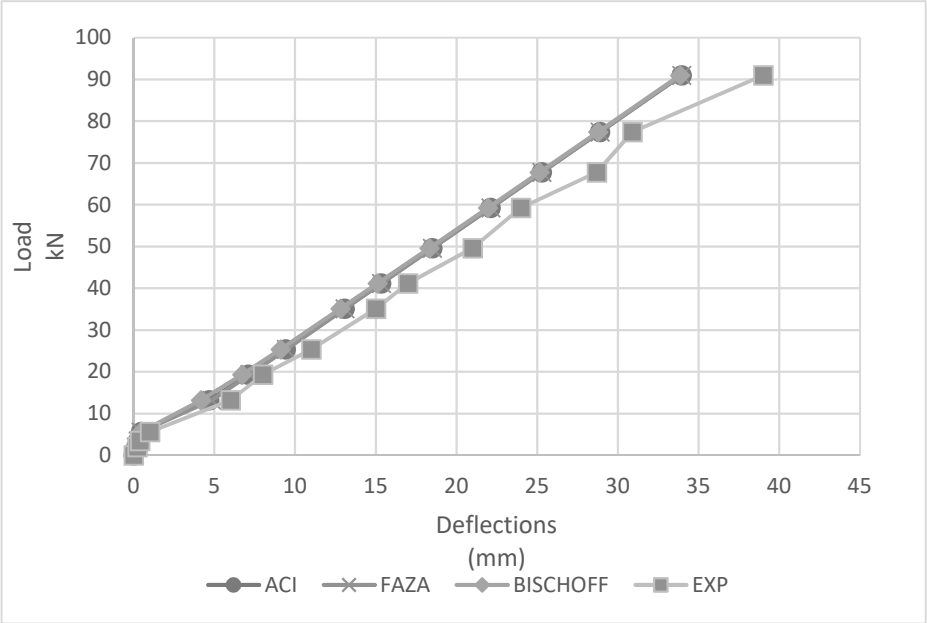

Figure 32 Comparison of deflections with different moment of inertia A25-3

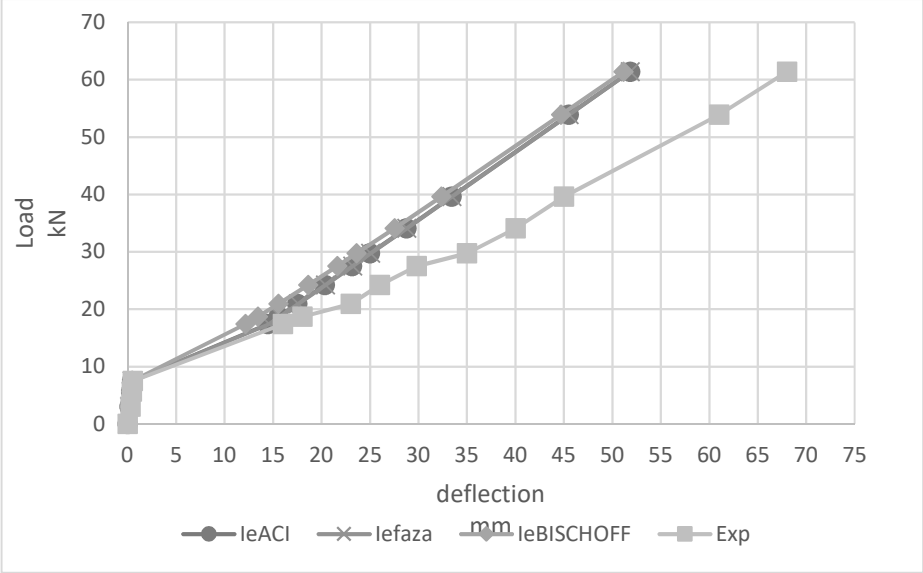

Figure 33 Comparison of deflections with different moment of inertia A45-1

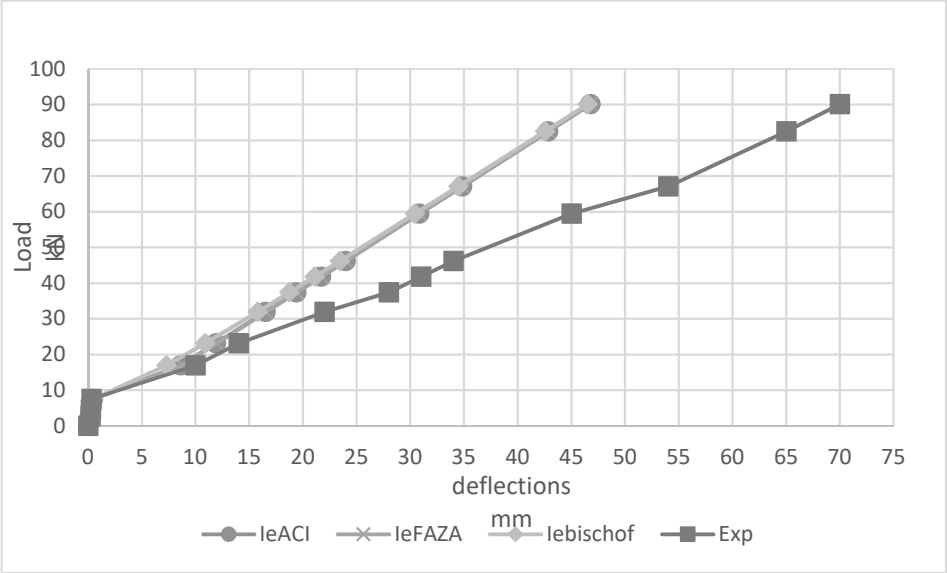

Figure 34 Comparison of deflections with different moment of inertia A45-2

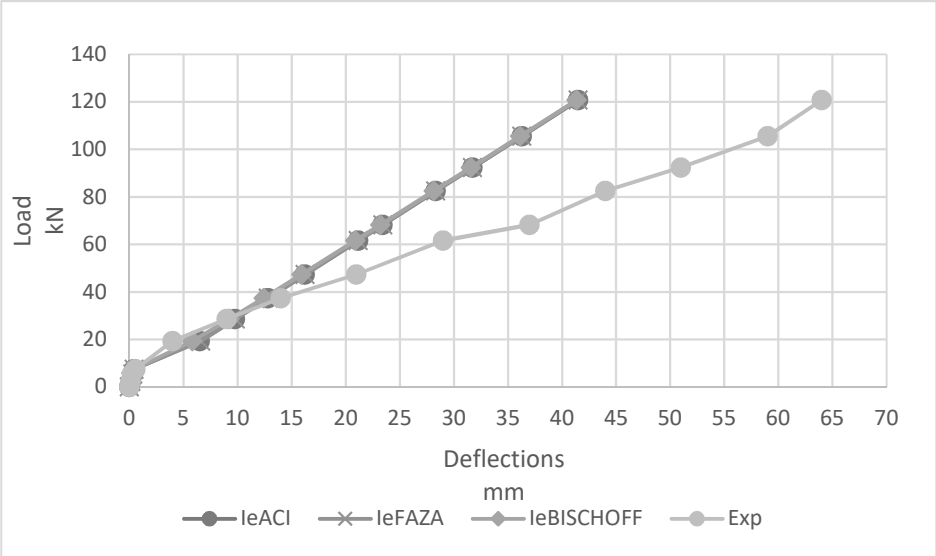

Figure 35 Comparison of deflections with different moment of inertia A45-3

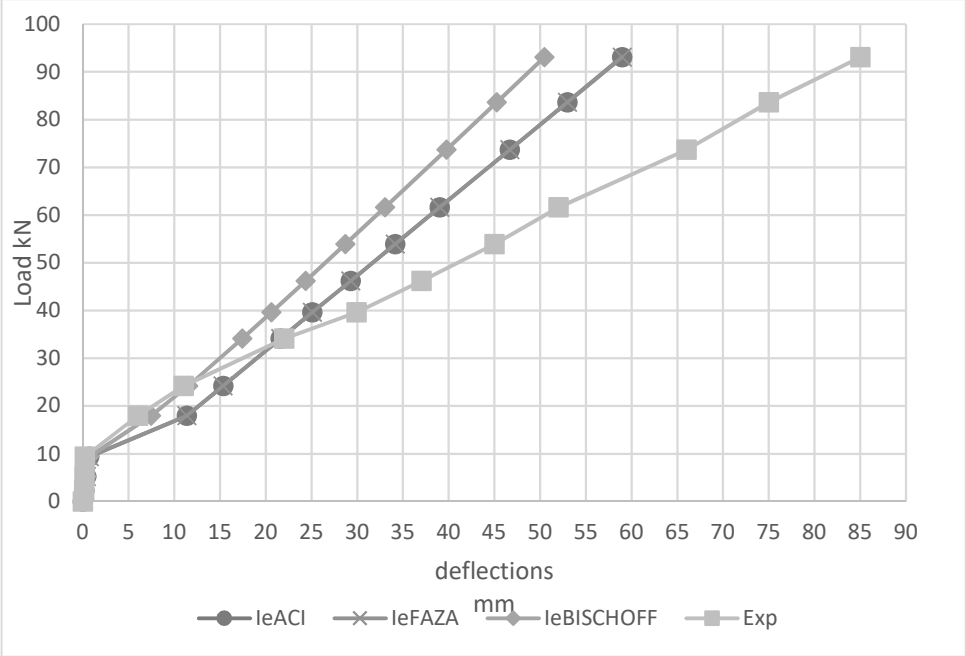

Figure 36 Comparison of deflections with different moment of inertia A70-1

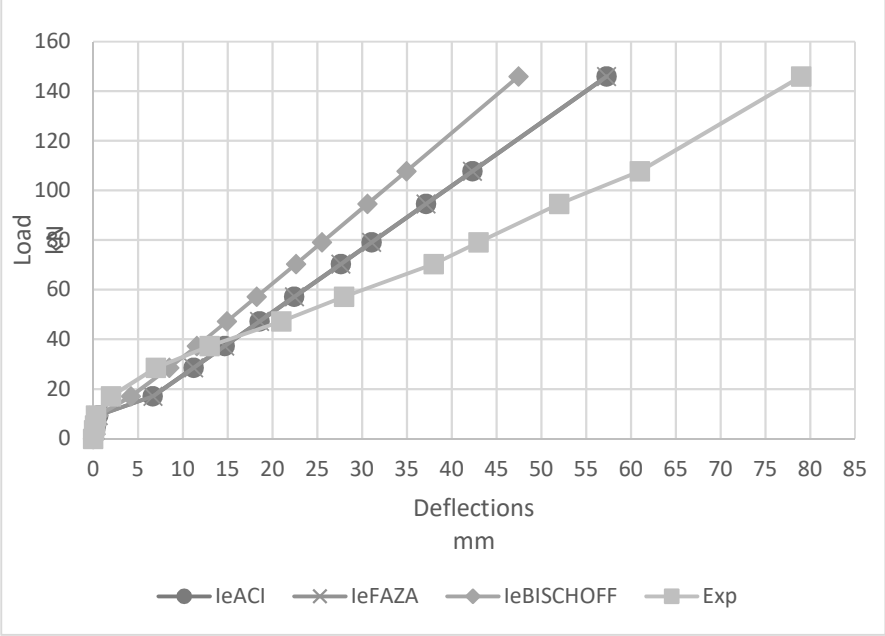

Figure 37 Comparison of deflections with different moment of inertia A70-2

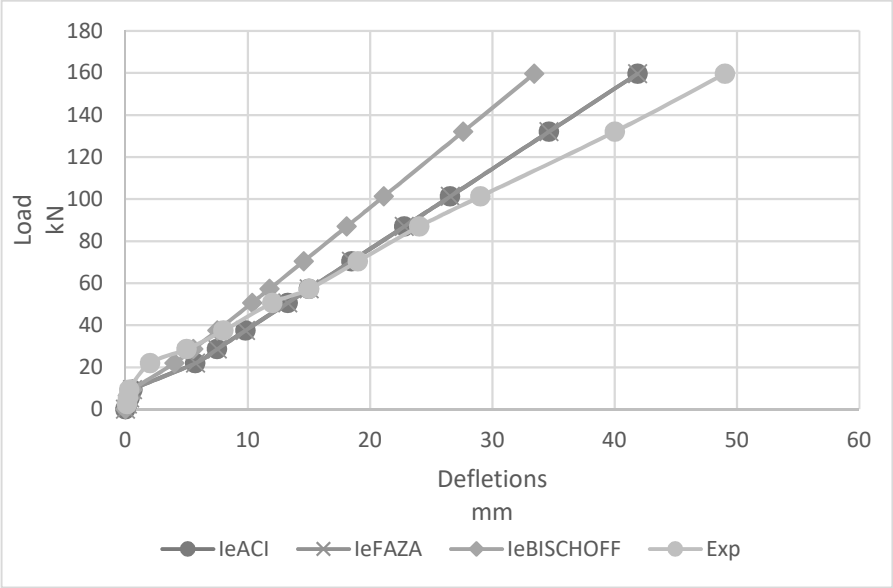

Figure 38 Comparison of deflections with different moment of inertia A70-3

As the difference between the different theoretical equation and the experimental result are quite different, the following graphs include a new equation with a modified equation.

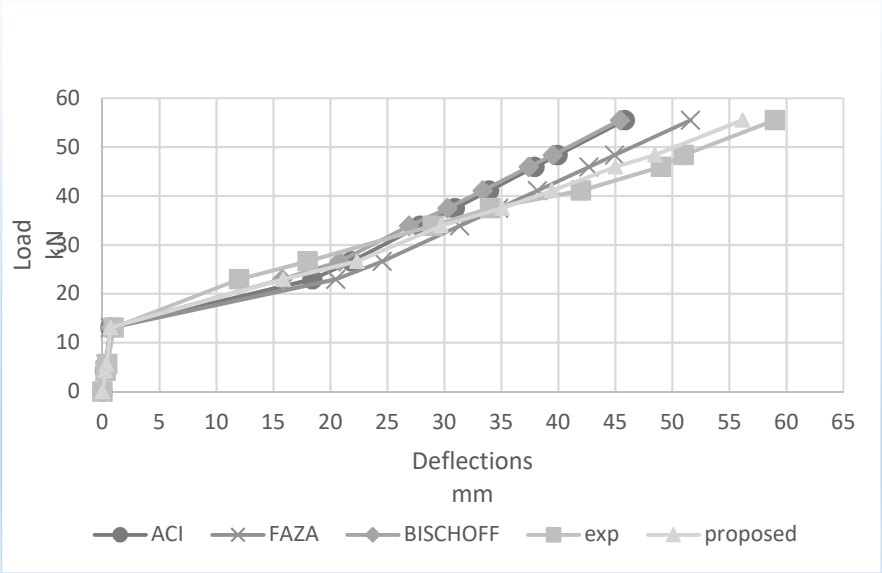

Figure 39 Comparison of deflections with different moment of inertia A25-1

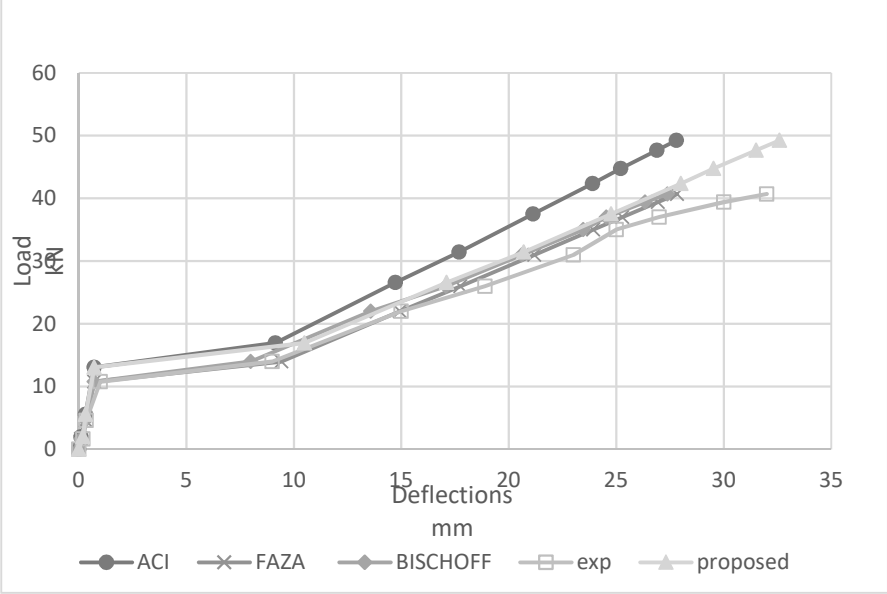

Figure 40 Comparison of deflections with different moment of inertia A25-2

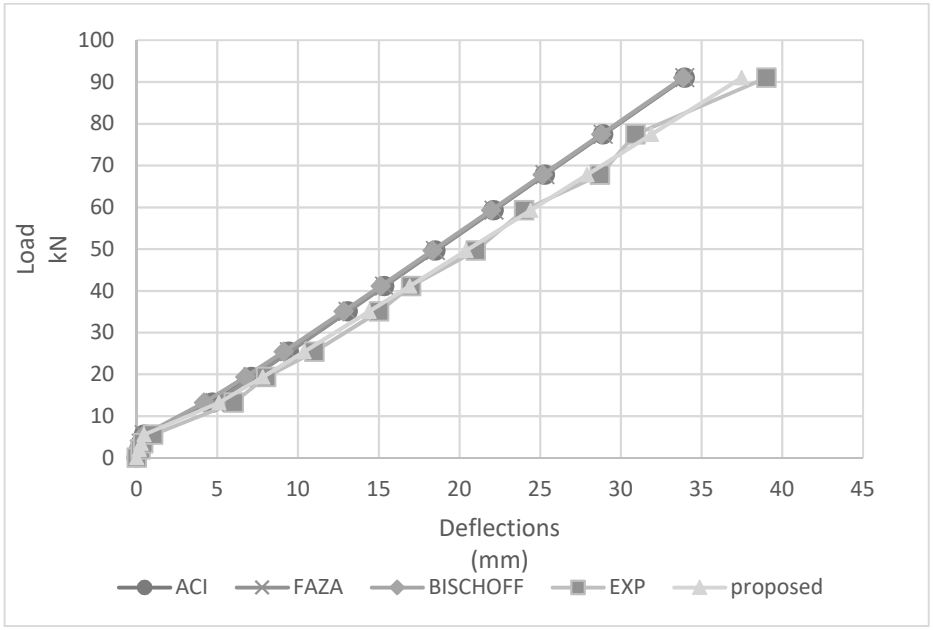

Figure 41 Comparison of deflections with different moment of inertia A25-3

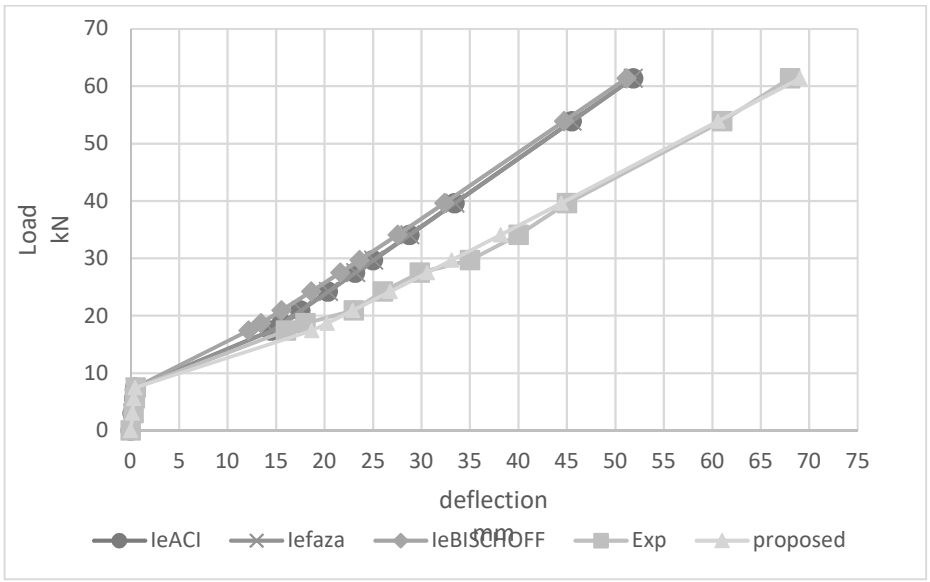

Figure 42 Comparison of deflections with different moment of inertia A45-1

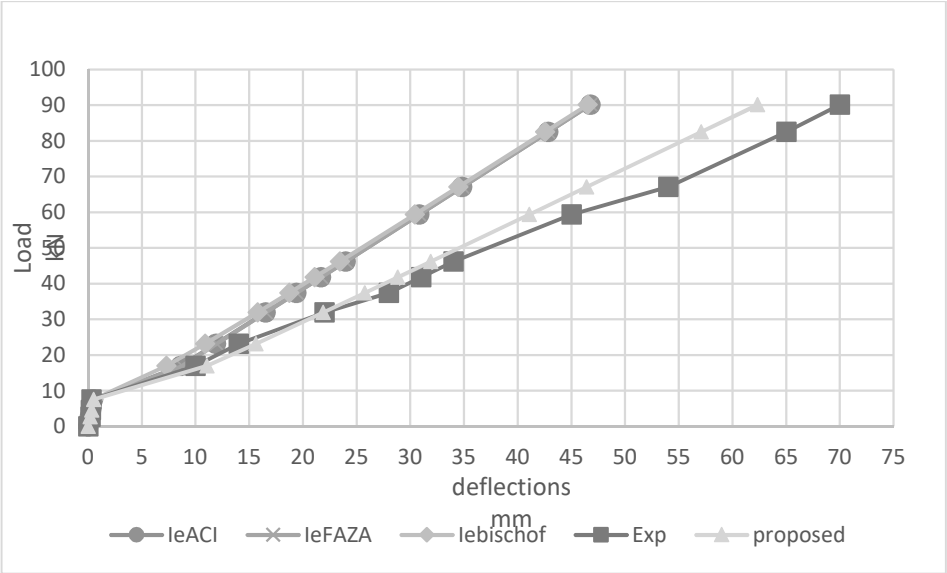

Figure 43 Comparison of deflections with different moment of inertia A45-2

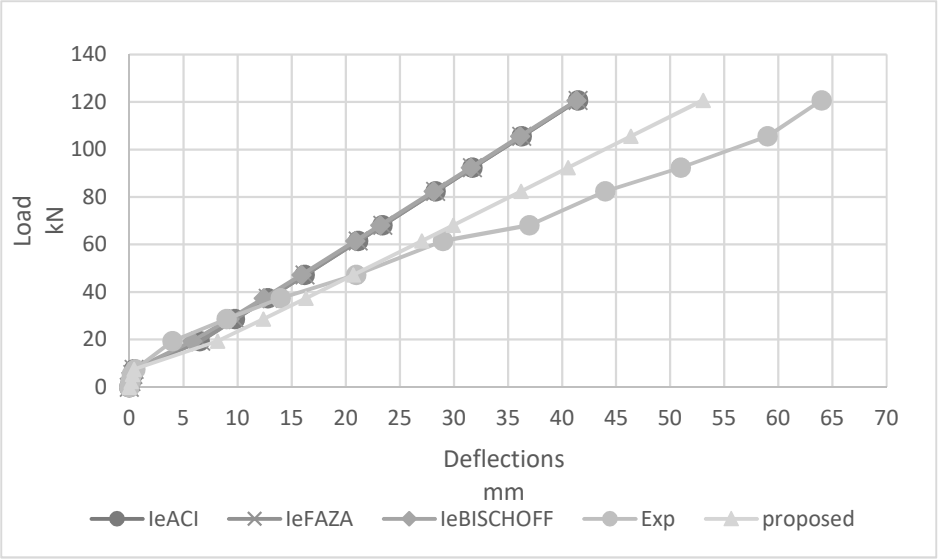

Figure 44 Comparison of deflections with different moment of inertia A45-3

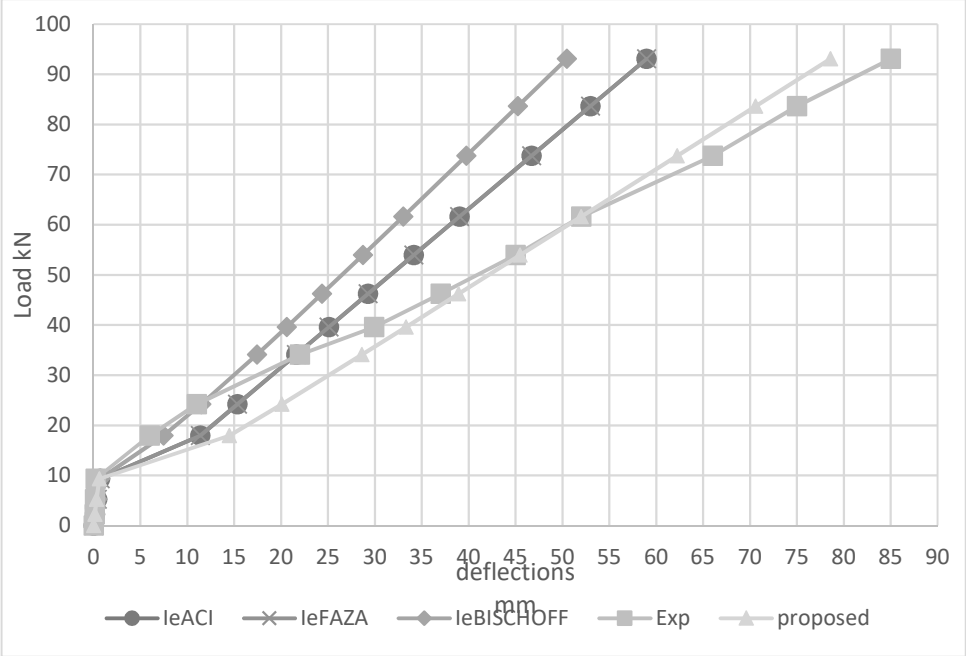

Figure 45 Comparison of deflections with different moment of inertia A70-1

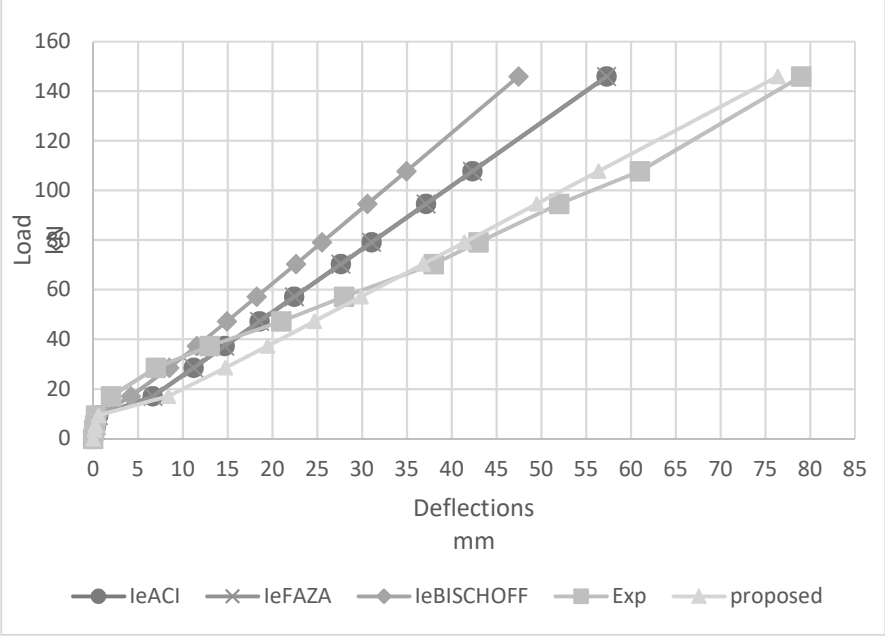

Figure 46 Comparison of deflections with different moment of inertia A70-2

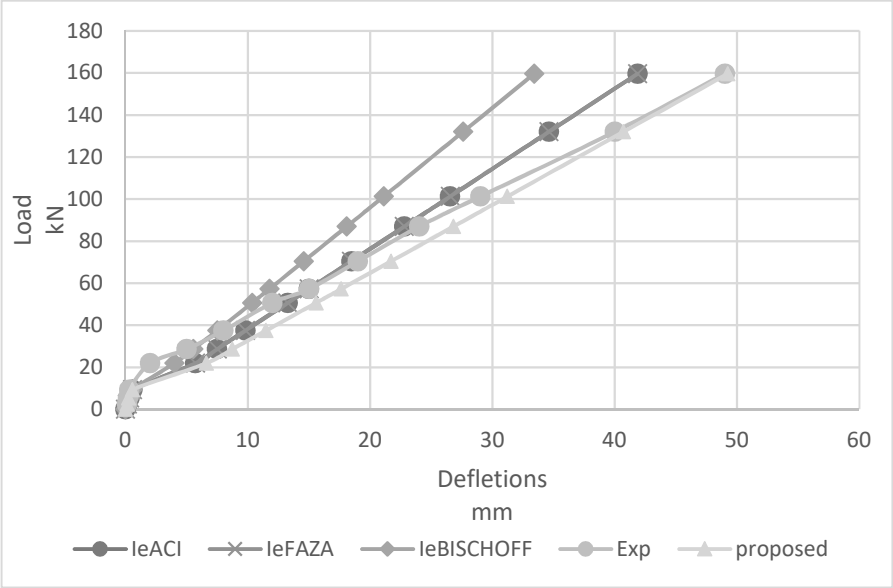

Figure 47 Comparison of deflections with different moment of inertia A70-3

5. Conclusions

This thesis investigated the flexural behavior of concrete beams reinforced with GFRP bars. The main point is to compare results obtained from theoretical equation and experimental data.

- The theoretical deflections are lower than the experimental results in all the specimens. While for series A25 and A45 the theoretical curves present similar results for the series A70 the deflections results with BISCHOFF'S equation are around 10% less then FAZA and ACI equations.
- Analysis of methods describe the quite different differences between the theoretical and experimental results, all methods gave too conservative value of the deflections so; the stiffness of section should be corrected. The reduction of the cracked section moment of inertia has quite significant effect for bending moment and deflection relationship. For this reason, a reduction coefficient of 0.75 is suggest to better describe the coincidence of the theoretical and experimental deflections curves, the range pass from 12% to 4%.

References

[1] **Nasim Udin .** Developments in fiber-reinforced polymer (FRP) composites for civil engineering . Woodhead Publishing 2013 number 45. ISBN 978-0-85709-234-2

[2] *Kim, Naaman & El-Tawil*, 2008

[3] **Hany Jawaheri Zadeh, Antonio De Luca, Antonio Nanni** Reinforced Concrete with FRP Bars. (Mechanics and design) January 1, 2014 . ISBN-13:978-0-415-77882-4

[4] **ACI Committee 440**.Report on fiber-reinforced polymer (FRP) reinforcement for concrete structures. ACI 440R-07,American Concrete Institute , Farmington Hills , MI(2007)

[5] **C.E. Bakis ,L.C. Bank,V.L. Brown,E. Cosenza,J.F.Davalos** and **J.J.Lesko**, et al. Fiber-reinforced polymer composites for construction : State-of-the art review.ASCE Journal of Composites for Construction 6 (2):73-87-(2002).

[6] **L.C. Bank**, Properties of FRP reinforcement for concrete. In fiber-reinforced-plastic (FRP) reinforcement for concrete structures: Properties and applications. Developments in civil engineering, ed. A.Nanni,42,59-86. Amsterdam:Elsevier(1993).

[7] **Hayder A.Rasheed** , Strengthening Design of Reinforced Concrete with FRP,2015 ISBN -13:978-1-4822-3558-6 (Hardback)

[8**] M.W.**1998. Stress analysis of fiber reinforced composite materials. New York :WCB/McGraw Hill.

[9**] A. Nanni.** Fiber-reinforced-plastic for concrete structures: Properties and applications. Amsterdam: Elsevier Science (1993).

[10] **A. Nanni,S. Rizkalla**, **C. E. Bakis**, J.O. Conrad, and A.A. Abdelrhman. Characterization of GFRP ribbed rod used for reinforced concrete construction Proceedings of the International Composites Exhibition (ICE-98), Nashville, TN, pp. 16A/1-6 (1998).

[11] **Wu, W. P.,** 1990, "Thermomechanical Properties of Fiber Reinforced Plastic (FRP) Bars," PhD dissertation, West. Virginia University, Morgantown, W.Va., 292 pp.

[12] http://www.gurzi.it/materiale/02EGJAG.pdf

[13] **Bootle, J.; Burzesi, F**.; and **Fiorini, L**., 2001, "Design Guidelines," *ASM Handbook*, V. 21, Composites, ASM International, Material Park, Ohio, pp. 388-395.

[14] **Kumahara,** S.; **Masuda, Y**.; and **Tanano, Y**., 1993, "Tensile Strength of Continuous Fiber Bar Under High Temperature," Fiber-Reinforced-Plastic Reinforcement for Concrete Structures—International Symposium, SP-138, A. Nanni and C. W. Dolan, eds., American Concrete Institute, Farmington Hills, Mich., pp. 731-742.

[15] **R.V. Balendran, W.E. Tang, H.Y. Leung, A. Nadeem,** 2004, "Flexural behavior of sand coated glass fibre reinforced polymer (GFRP) bars in concrete ".

[16] **Maher A. Adam, Mohamed Said, Ahmed A. Mahmoud, Ali S. Shanour,** 2015, "Analytical and experimental flexural behavior of concrete beams reinforced with glass fiber reinforced polymers bars".